International Advance Journal of Engineering Research (IAJER)
Volume 3, Issue 9 (September- 2020), PP 01-30
ISSN: 2360-819X
www.iajer.com

Research Paper **Open Access**

Registration of Pre-Seismic Radio Signals Related To The Russian And Jamaican Earthquakes With The RDF System Developed By The Radio Emissions Project

Daniele Cataldi[1,2], Valentino Straser[3], Gabriele Cataldi[1], Giampaolo Giocacchino Giuliani[2], Zamri Zainal Adibin[4]

[1]*Radio Emissions Project – Lariano, Rome, Italy*
[2]*Foundation "G. Giuliani ONLUS", L'Aquila, Italy;*
[3]*Geoplasma Research Institute – Colorado (USA);*
[4]*Radio Cosmology Research Lab, Department of Physics, University of Malaya – Kuala Lumpur, Malaysia.*

ABSTRACT
The authors are engaged in solar activity monitoring (since 2011) and in Earth's geomagnetic background monitoring (since 2009), in search of natural electromagnetic signals that can be related to potentially destructive tectonic phenomena. Thanks to this new scientific approach it has been possible to correlate some natural radio emissions to the potentially destructive seismic activity that is recorded both on a global scale and in Italy(G. Cataldi et al., 2013-2017; G. Cataldi et al., 2019; G. Cataldi, 2020; D. Cataldi et al., 2014; D. Cataldi et al., 2017; D. Cataldi et al., 2019-2020; T. Rabeh et al., 2014; V. Straser, 2011-2012; V. Straser et al., 2014-2017; V. Straser, 2017; V. Straser et al., 2019-2020; F. Di Stefano et al., 2020).In 2017 the authors created the first worldwide multi-parametric monitoring network dedicated to seismic prediction that can simultaneously monitor: the environmental radiofrequency in the SELF-LF band (> 0-96 kHz) through RDF (Radio Direction Finder) technology and the flow of $Radon_{222}$ gas, in order to perform a crustal diagnosis in real-time that is able to establish if the conditions are in place for a seismic event to occur. The first results of this new scientific approach dedicated to local and global seismicity have allowed the authors to obtain very encouraging results in the field of seismic prediction (D. Cataldi et al., 2019-2020; V. Straser et al., 2018-2020; F. Di Stefano et al., 2020).

Keywords: EarthquakePrevision, Radio DirectionFinding, RDF,Electromagnetic Monitoring, Seismic Electromagnetic Precursor.

I. INTRODUCTION

The pre-seismic radio emissions, or rather, the Seismic Electromagnetic Precursors (SEPs) are natural radio emissions that precede seismic events of various sizes and those scientists have been able to observe on several occasions through various types of electronic equipment since the end of 19th century (J. Milne, 1890). Recent studies have made it possible to establish that there are two large families of SEPs (G. Cataldi, 2020; V. Straset et al., 2020; D. Cataldi et al., 2020):

1. Seismic Electromagnetic Precursors (SEPs) or **Local SEPs**;
2. Seismic Electromagnetic Precursors (SEPs) or **Non-local SEPs**.

The first family (Local SEPs) includes emissions/phenomena of an electromagnetic nature that interact with the Earth's geomagnetic field and that are observed in interplanetary space: for this reason the authors have defined them as "Interplanetary Seismic Precursors" (ISPs). All geomagnetic emissions are also part of the first family resulting from the impact that solar activity has on the Earth's geomagnetic field and which, for this reason, have been defined as "Seismic Geomagnetic Precursors" (SGPs):

- Interplanetary Seismic Precursors (ISPs)(Non-local SEPs):
- variations in the density and velocity of the solar ion flux (solar wind);
- increases in the solar wind dynamic pressure;
- CIR (Co-rotating Interaction Regions);

- CMEs (Coronal Mass Ejections);

➢ Seismic Geomagnetic Precursors (SGPs)(Non-local SEPs):

- variations of the Earth's geomagnetic field on any of the vector / angular components;
- polar electromagnetic emissions;
- appearance of ELF Storms;
- Variation of the geomagnetic indices.

The second family (Non-local SEPs), on the other hand, includes all those pre-seismic radio emissions that have no direct link with the Earth's geomagnetic field or with solar activity as they are produced in the Earth's crust through the phenomenon of piezoelectricity following accumulation tectonic stress on the rocks that are deformed mechanically, as suggested by many researchers since the second half of the twentieth century and the authors (G. Cataldi, 2020; D. Cataldi et al., 2020; V. Straser et al., 2020; F. Freund, 2002; D. Finkelstein et al., 1973):

➢ Seismic Electromagnetic Precursors (SEPs) (Local SEPs)

- broadband pre-seismic electromagnetic emissions not directly related to the Earth's geomagnetic field.

The first family of electromagnetic seismic precursors (Local SEPs) can be detected instrumentally through the use of radio receivers tuned in the SELF-LF band (>0-96 kHz). The second family of electromagnetic seismic precursors (Non-local SEPs) can be detected instrumentally through the use of artificial satellites (ISPs) or through the use of magnetometers located on any point of the Earth's surface (SGPs) tuned in the SELF-ELF band (>0-30 Hz); (**Fig. 1**).

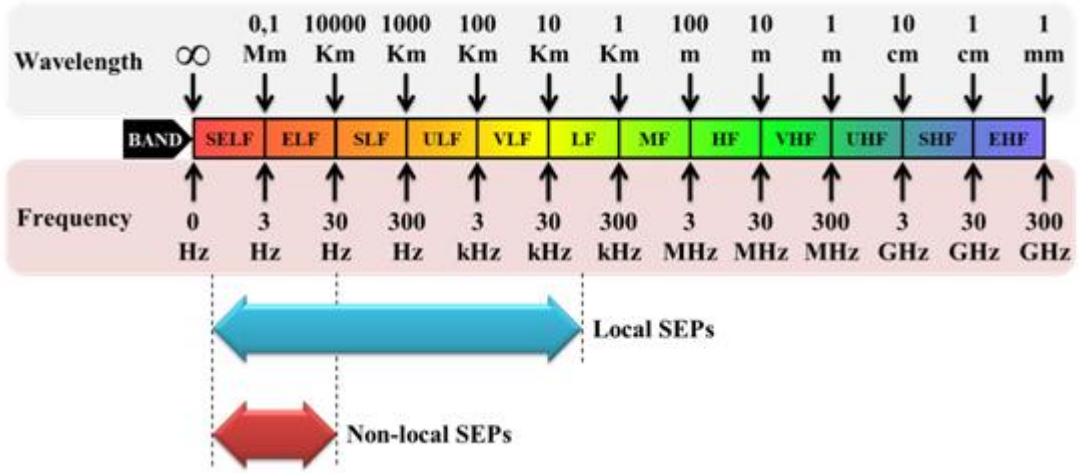

Fig. 1 – Bandwidths of Seismic Electromagnetic Precursors (SEPs) compared.

In the image above, the bandwidths of "Local" and "Non-local" SEPs have been compared. Due to the attenuation produced by the propagation medium (air-ground), the bandwidth of the Local SEPs is progressively reduced based on the distance from which they are picked up and in an inversely proportional way to their wavelength. Credits: Gabriele Cataldi, Daniele Cataldi, Radio Emissions Project.

Since the production mechanism of the "Local SEPs" provides for a direct action of the tectonic stress on the crystal grid of the rocks included in the fault planes of the Earth's surface areas seismically active (direct piezoelectric effect), it is evident that this electromagnetic source could be used to identify seismic epicenters before a seismic event occurs. The authors worked on this in 2016. In fact, Gabriele Cataldi and Daniele Cataldi (founders of the Radio Emissions Project) in 2017 developed a "continuous" environmental electromagnetic monitoring network implemented with "Radio Direction Finding" (RDF) technology: technology that allows to establish the azimuth of the electromagnetic signals arriving at a specific RDF monitoring station (V. Straser et al., 2018). Using a network of at least 2 or 3 RDF monitoring stations it is possible to understand, through the triangulation method, where any electromagnetic source observed in a given bandwidth is geographically located.

The RDF monitoring stations built by the authors are currently located in Italy and Malaysia and represent the first RDF monitoring network dedicated to the prediction of potentially destructive earthquakes.

This network made it possible to identify in advance seismic epicenters of potentially destructive earthquakes even 18000km away from the nearest RDF station. (D. Cataldi et al., 2019-2020; V. Straser et al., 2018-2020).

This work presents the results of the RDF monitoring conducted on three M7+ seismic events recorded between January 28, 2020 and March 25, 2020 (**Fig. 2**):

- **Mw 7.7**earthquake, localized at 125 km NNW of Lucea, Jamaica, GPS (Global Positioning System) position: 19.440°N 78.755°W (depth: 10.0 km), recorded onJanuary 28, 2020 at 19:10:25 UTC.
- **Mw 7.0** earthquake,localized at 94 km ENE of Kuril'sk, Russia, GPS (Global Positioning System) position: 45.616°N 148.959°E (depth: 143.0 km), recorded on February 13, 2020 at10:22:44 UTC.
- **Mw 7.5** earthquake,localized at 221 km SSE of Severo-Kuril'sk, Russia, GPS (Global Positioning System) position: 48.964°N 157.696°E (depth: 57.8 km), recorded on March 25, 2020at 02:49:25 UTC.

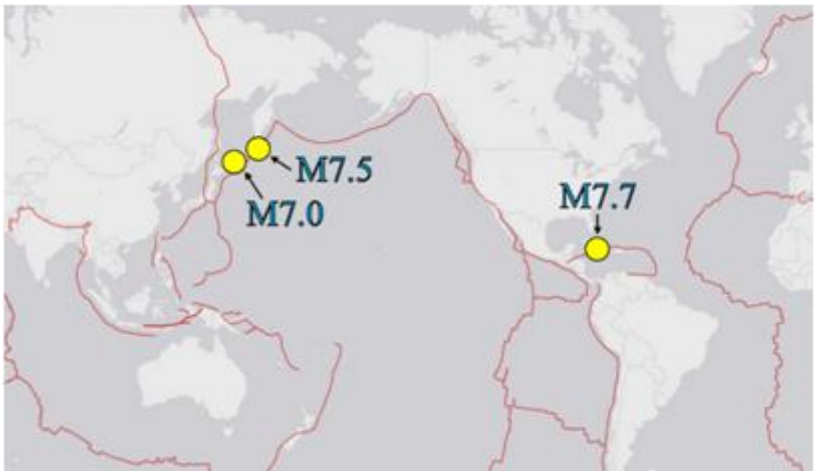

Fig. 2 – Epicentri dei tre eventi sismici potenzialmente distruttivi analizzati in questo lavoro.

Nella cartina in alto sono visibili gli epicentri sismici dei seguenti terremoti: M7.7 – Jamaica earthquake, registrato il 28 Gennaio 2020 alle ore 19:10 UTC; M7.0 – Russia earthquake, registrato il 13 Febbraio 2020 alle ore 10:33 UTC; M7.5 – Russia Earthquake, registrato il 25 Marzo 2020 alle ore 02:49 UTC.Credits: USGS.

II. METHODS AND DATA – RDF SYSTEM

To carry out this study, was used the monitoring data provided by the RDF (Radio Direction Finding) network located between Italy and Malaysia: a network developed by Gabriele Cataldi and Daniele Cataldi (Radio Emissions Project) between 2017 and 2020 with the help of the "Foundation G. Giuliani ONLUS" and the University of Malaya. This monitoring network will undergo progressive expansion over the next few years. The survey stations considered in this study were the following:

- Lariano RDF Station, Rome, Italy – RDF Monitor 1. Radio Emissions Project.GPS (Global Positioning System): Lat: 41.728799 N, Long: 12.843205 E.
- Lariano RDF Station, Rome, Italy– RDF Monitor 2. Radio Emissions Project.GPS (Global Positioning System): Lat: 41.728799 N, Long: 12.843205 E.
- Ripa-Fagnano RDF Station, L'Aquila, Italia. Foundation G. Giuliani ONLUS". Radio Emissions Project Network.GPS (Global Positioning System):Lat: 42.265690 N, Long: 13.583793 E
- Kuala Lumpur RDF Station, Malesia (University of Malaya). Radio Emissions Project Network. GPS (Global Positioning System):Lat: 3.123060 N, Long: 101.653044 E.

All RDF electromagnetic monitoring stations are equipped with a radio receiver system capable of working efficiently over a wide bandwidth (SELF-LF band: >0-96kHz). This detection system was designed and developed by the Radio Emissions Project in 2016 and made operational in 2017. Each single RDF station consists of (**Fig. 3**):

- two loop antennas oriented along the North-South and East-West axes, and orthogonally to each other;
- a dual channel radio receiver (RDF prototype) that has an amplification of 200x (46dB);

- a computer that is able to analyze the stereo audio signal coming out of the receiver through an ADC of at least 24 bits and with a sampling frequency of 192kHz.

The radio signals received, after being filtered and amplified, are sent to a computer to be processed electronically. In this phase, a computer calculates the azimuth of the captured electromagnetic signals by comparing the electrical values supplied by the two loop antennas and creates a dynamic spectrogram where each electromagnetic signal is associated with a color corresponding to the calculated azimuth (V. Straser et al., 2019-2020; D. Cataldi et al., 2019) (**Fig.4**). In summary, on the spectrogram is condensed the following information on the monitored radiofrequency in relation to the time variable:

- frequency;
- azimuth (color scale, 256 colors), with a maximum resolution of 1.4°
- intensity (indicated by the color saturation level associated with azimuth);
- emissionpeaks;

This information allows to obtain spectral imprints of all electromagnetic emissions captured by each single RDF station.

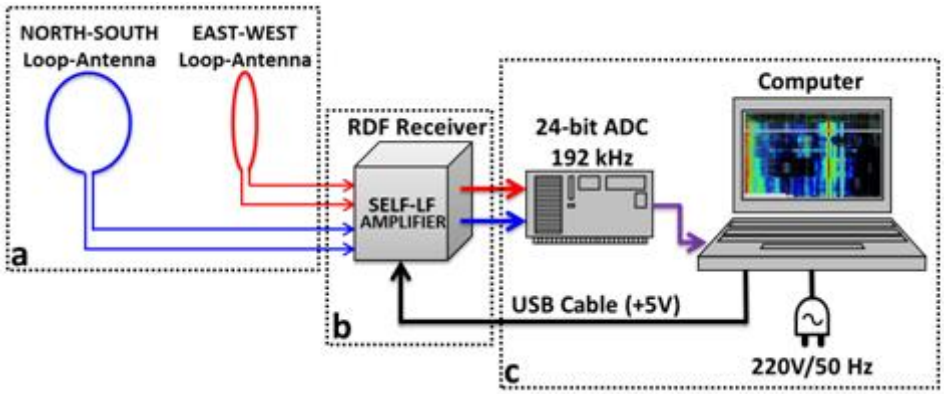

Fig. 3 – RDF (Radio Direction Finding) technology.

The figure above shows a simplified diagram of the electrical connections present in a "continuous" electromagnetic monitoring station based on RDF (Radio Direction Finding) technology. a) the loop antennas oriented along the North-South and East-West axes are oriented orthogonally to each other; b) the RDF receiver is a prototype designed by Gabriele Cataldi in 2016 which is powered directly through the USB socket of the computer; c) the computer system responsible for processing the radio signals captured by the loop antennas is equipped with a 24-bit ADC that provides a sampling of 192 kHz. Credits: Gabriele Cataldi, Daniele Cataldi, Radio Emissions Project.

Having established the exact position of each RDF station, the azimuth of the electromagnetic emissions captured through the RDF monitoring network was analyzed to determine the planimetric coordinates of any electromagnetic source through the triangulation of the azimuth data provided by the system. The determination of the planimetric coordinates of the source is carried out manually by the authors since the network is not equipped with an automatic (computerized) triangulation system, even if the future developments of the network continue in this direction..

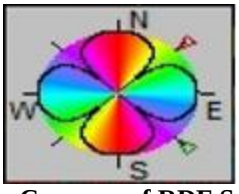

Fig. 4 – Compass of RDF System.

In the image on the left is visible the compass of the RDF System which is located inside the spectrograms. It indicates the gradations of color (256 tones) associated with the azimuth direction of the electromagnetic signals collected in relation to the four cardinal points (N, S, E, W). The black line in the shape of a four-leaf clover represents the diagram of the sensitivity of the RDF antenna which is made up of two loop antennas aligned orthogonally to each other (that's why 4 lobes are observed) and in the direction of the N-S and

E-W directrix; while the two small triangles (one green and one red) represent the direction along which the antenna has its least sensitivity. Credits: Radio Emissions Project.

The electromagnetic signals highlighted by the RDF system that have been correlated to the three M7+ seismic events analyzed in this work appeared, from a spectrographic point of view, well detached from the natural electromagnetic background, with a precise spectral imprint (azimuthal variation associated with a chromatic scale) and therefore they were clearly distinguishable from the natural background (natural noise).

2.1 - Methods and data – M7.7 Jamaican earthquake

On January 28, 2020, at 19:10:25 UTC, was recorded an earthquake of magnitude Mw 7.7 located at 125km NNW of Lucea, Jamaica, with GPS (Global Positioning System) position of: 19.440°N 78.755°W and at a depth of 10.0 km. Considering the epicentral position of the Jamaican earthquake, the position of the RDF monitoring stations and their related azimuth color grid, the azimuth possessed by the pre-seismic electromagnetic signals related to the seismic epicenter of the Jamaican earthquake can be easily traced: radio emissions generated through the direct piezoelectric effect (**Fig.5**):

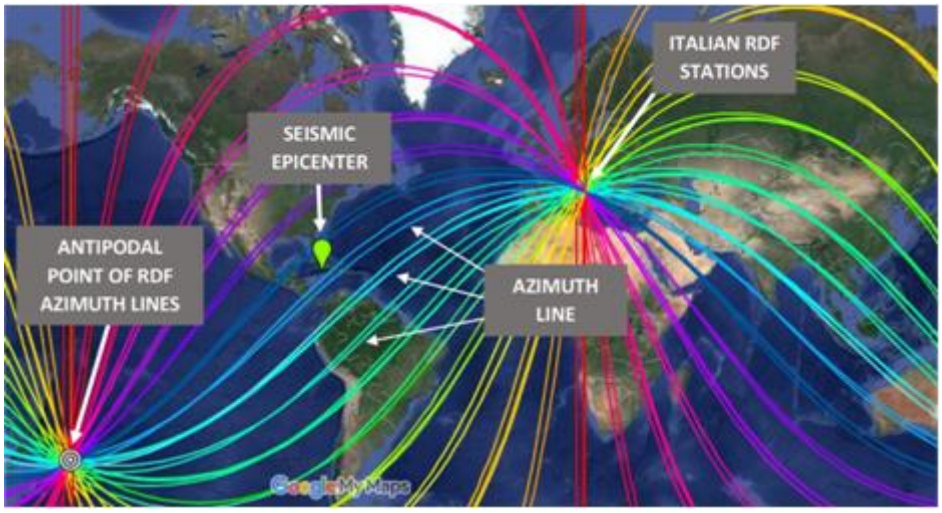

Fig. 5 – Azimuth grid analysis of the RDF monitoring network related to Jamaican M7.7 earthquake.

The image above shows the colorimetric map of the azimuth grid connected to the RDF monitoring network developed by the Radio Emissions Project in collaboration with the Permanent Foundation G. Giuliani ONLUS. The green marker represents the epicenter of the Jamaican M7.7 earthquake which occurred on January 28, 2020 at 19:10:25 UTC. It is evident that, compared to the RDF monitoring network located on the Italian territory, the epicenter of the Jamaican earthquake is located between the light blue and blue azimuth: this suggests that if through the direct piezoelectric effect were generated pre-seismic electromagnetic emissions in the focal zone of the Jamaican earthquake, these would appear on the RDF spectrograms as light blue-blue spectrographic traces. Credits: Gabriele Cataldi, Daniele Cataldi, Radio Emissions Project.

The RDF monitoring network, in accordance with what has been stated, was able to detect electromagnetic signals compatible with the azimuth of the Jamaican seismic epicenter. The first data provided by the RDF monitoring network are those relating to 25 January 2020 at 18:50 UTC, recorded by the RDF station of Lariano (RM) (RDF Monitor 1), where the appearance of bluish-type signals occurred very low frequency (0.001 Hz; SELF band), right on the geomagnetic band. At 08:30 UTC on 26 January 2020, the RDF station of Lariano (RM) detected other electromagnetic signals with the same azimuth but at a frequency between 0.05 and 0.5 Hz: these signals remained visible until 11:30 UTC of 26 January 2020 (**Fig. 6**)
The time data and frequency of electromagnetic signals detected by the RDF monitoring network with azimuth overlapping that of the Jamaican seismic epicenter are summarized below:

- Frequency 0.001 Hz — Time: 18:50 UTC — Date: January 25, 2020.
- Frequency 0.001 Hz — Time: 01:30 UTC — Date: January 28, 2020.

- Frequency 0.05 Hz — Time: 08:30 UTC — Date: January 26, 2020.
- Frequency 0.5 Hz — Time: 11:30 UTC — Date: January 26, 2020.

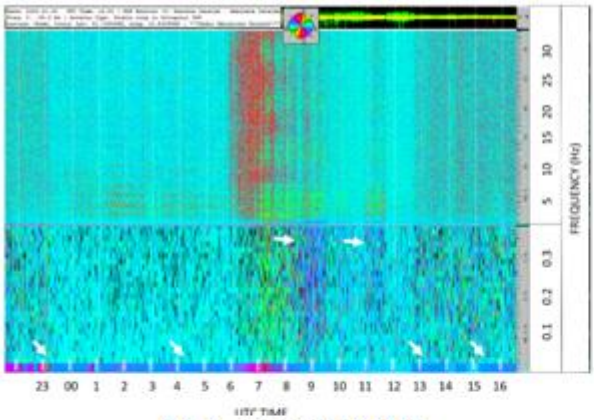

Fig. 6 – January 26, 2020.

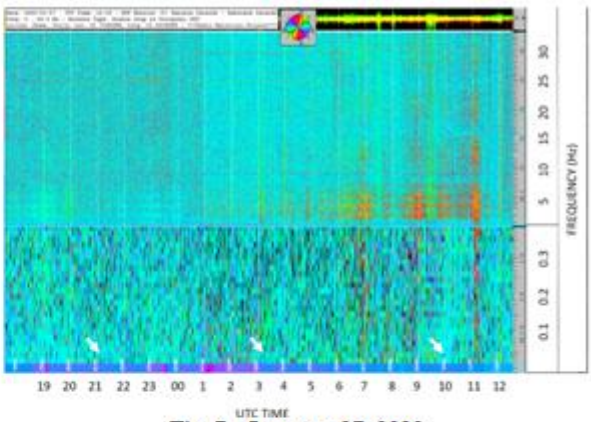

Fig. 7– January 27, 2020

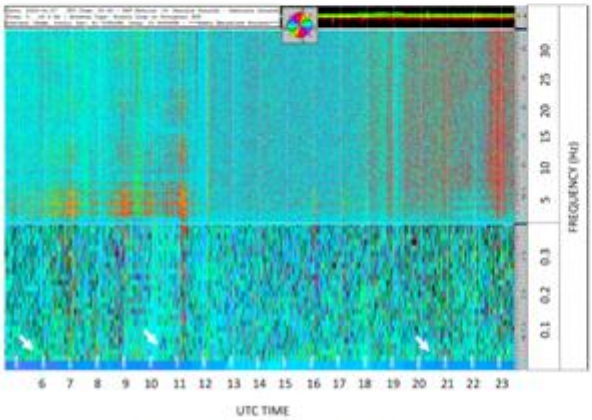

Fig. 8 – January 27, 2020

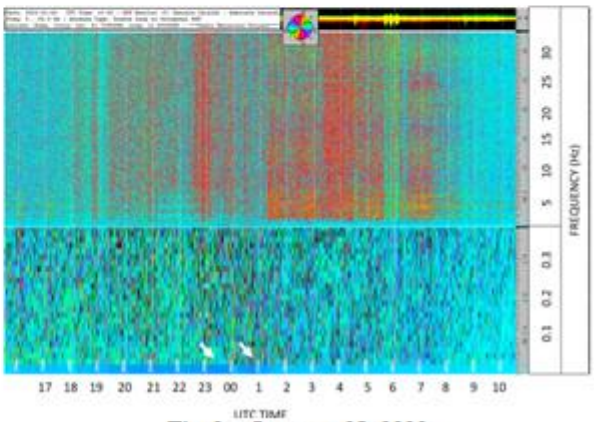

Fig. 9 – January 28, 2020

Fig. 6-9 – Dynamic spectrograms made by the RDF station of Lariano (RM), Italy.

The dynamic spectrograms above were made by the RDF station in Lariano (RM) (RDF Monitor 1) between 26 and 28 January 2020. The white arrows indicate the pre-seismic electromagnetic signals that have an azimuth compatible with the epicenter of the Jamaican earthquake. The UTC time is shown on the X axis relating to the recording of the spectrogram: this proceeds from right to left. The frequency of the monitored radio band is indicated on the Y axis: this is expressed in Hz. The spectrogram has been divided into two portions: the upper part highlights the ELF band; the lower part highlights the SELF band. Credits: Gabriele Cataldi, Daniele Cataldi, Radio Emissions Project.

Further confirmations on the azimuth of the electromagnetic signals related to the Jamaican M7.7 earthquake were provided by the RDF station of Ripa-Fagnano (AQ), managed by the G. Giuliani Permanent Foundation and by the RDF stations of Lariano (RM) (monitor 1 and 2). The monitoring data of the RDF station of Ripa-Fagnano (AQ) have in fact highlighted the presence of radiofrequency with azimuth compatible with the epicenter of M7.7 Jamaican earthquake, starting from 23:30 UTC on January 27, 2020, up to at about 13:30 UTC on January 28, 2020, the day the earthquake occurred (at 19:10:25 UTC), as shown in **Fig. 10**. The electromagnetic emission recorded by the Ripa-Fagnano RDF station had a variable frequency: 0.05-12 Hz (close to the limit of the band displayed in the RDF spectrogram). The first RDF station in Lariano (RM) (monitor 1), Italy, recorded radio signals with azimuth compatible with the epicenter of the Jamaican M7.7 earthquake around 06:45 UTC on January 27, 2020 (as shown in **Fig. 11**) , when a bluish increase appeared on the spectrogram of the second RDF station in Lariano (RM), Italy. This signal, extended to a wide frequency, highlighted the azimuth of the Jamaican seismic epicenter (**Fig. 5**). In this case, the frequency of the electromagnetic signals was between 0.1 Hz and 5 Hz (near the lower instrumental limine of the RDF station) (**Fig. 12**). Further increases, recorded by the same RDF station in Lariano (RM), were observed at the same frequency, between 06:10 UTC and 12:00 UTC on January 28, 2020 (**Fig. 12**).

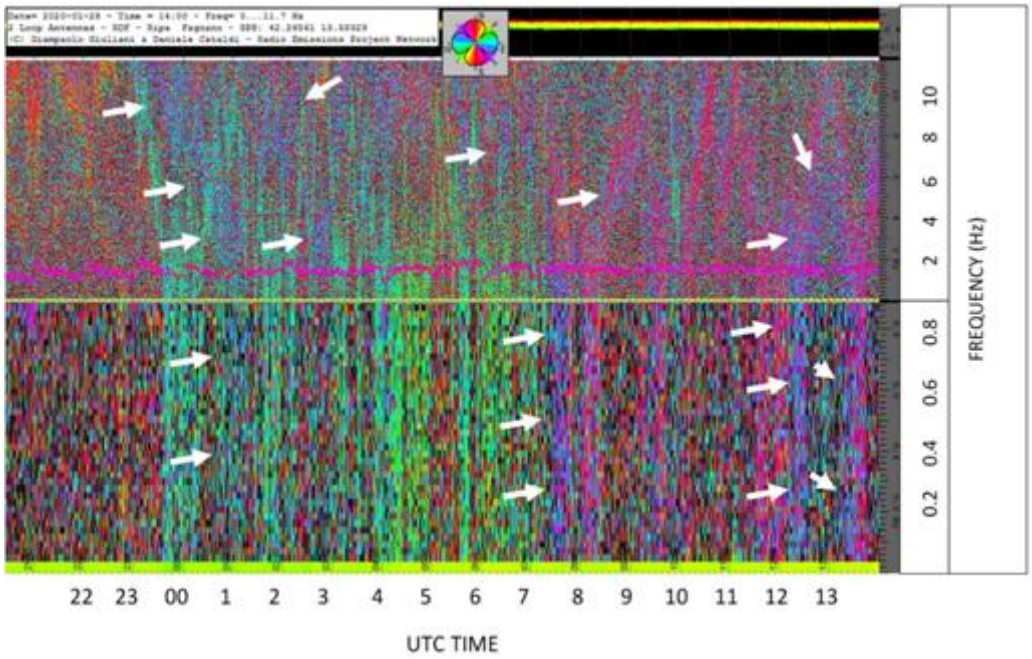

Fig. 10 – Dynamic spectrogram created by Ripa-Fagnano RDF station (AQ), Italy.

The dynamic spectrogram visible above was made by the Ripa-Fagnano RDF monitoring station (AQ) between 27 and 28 January 2020. The white arrows indicate the pre-seismic electromagnetic signals that have an azimuth compatible with the epicenter of the Jamaican earthquake.The white arrows indicate the pre-seismic electromagnetic signals that have an azimuth compatible with the epicenter of the Jamaican earthquake. The UTC time is shown on the X axis relating to the recording of the spectrogram: this proceeds from right to left. The frequency of the monitored radio band is indicated on the Y axis: this is expressed in Hz. The spectrogram has been divided into two portions: the upper part highlights the ELF band; the lower part highlights the SELF band. Credits: Gabriele Cataldi, Daniele Cataldi, Radio Emissions Project.

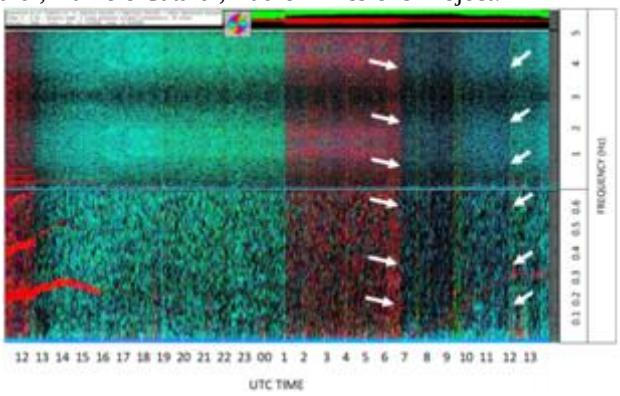

Fig. 11 – Dynamic spectrogram created by the first RDF station of Lariano (RM), Italy.

The dynamic spectrogram visible on the left was created by the first RDF monitoring station of Lariano (RM) on January 27, 2020. The white arrows indicate the pre-seismic electromagnetic signals that have an azimuth compatible with the epicenter of the Jamaican earthquake.The white arrows indicate the pre-seismic electromagnetic signals that have an azimuth compatible with the epicenter of the Jamaican earthquake. The UTC time is shown on the X axis relating to the recording of the spectrogram: this proceeds from right to left. The frequency of the monitored radio band is indicated on the Y axis: this is expressed in Hz. The spectrogram has been divided into two portions: the upper part highlights the ELF band; the lower part highlights the SELF band. Credits: Gabriele Cataldi, Daniele Cataldi, Radio Emissions Project.

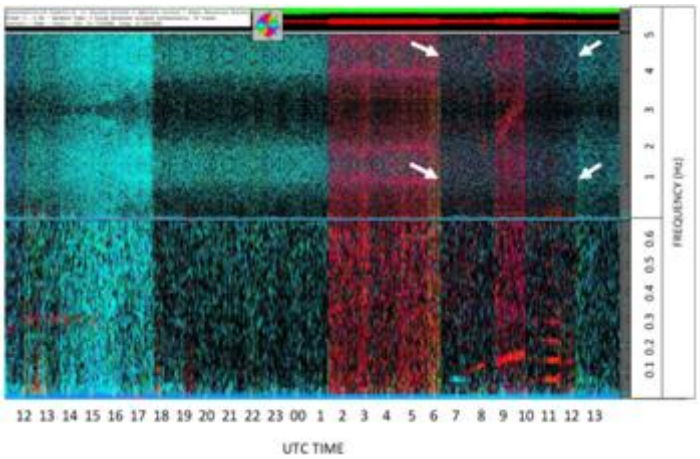

Fig. 12 – Dynamic spectrogram created by the second RDF station of Lariano (RM), Italy.

The dynamic spectrogram visible on the left was created by the second RDF monitoring station of Lariano (RM) on January 27, 2020. The white arrows indicate the pre-seismic electromagnetic signals that have an azimuth compatible with the epicenter of the Jamaican earthquake.The white arrows indicate the pre-seismic electromagnetic signals that have an azimuth compatible with the epicenter of the Jamaican earthquake. The UTC time is shown on the X axis relating to the recording of the spectrogram: this proceeds from right to left. The frequency of the monitored radio band is indicated on the Y axis: this is expressed in Hz. The spectrogram has been divided into two portions: the upper part highlights the ELF band; the lower part highlights the SELF band. Credits: Gabriele Cataldi, Daniele Cataldi, Radio Emissions Project.

By triangulating the azimuth data provided by the RDF monitoring network between 26 and 28 January 2020, it was possible to confirm that the radio signals captured have azimuth compatible with that of the Jamaican seismic epicenter.

2.2 -Methods and data – M7.0 Russian earthquake

On February 13, 2020, at 10:22:44 UTC, an earthquake of magnitude Mw 7.0 was recorded at 94km ENE of Kuril'sk, Russia, with GPS (Global Positioning System) position: 45.616°N 148.959°E and 143.0 km of depth (**Fig. 13**).

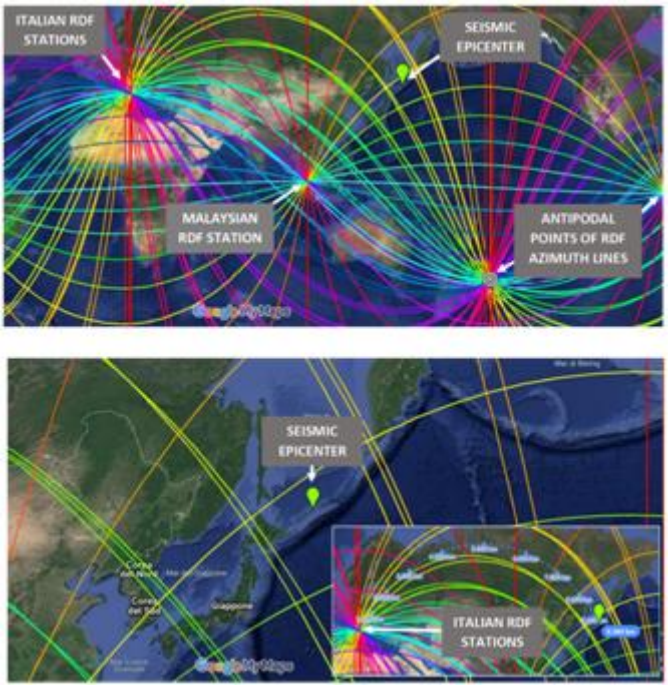

Fig. 13 – Analysis of the azimuth grid of the RDF monitoring network correlated to M7.0 Russian earthquake.

The image on the left shows the colorimetric map of the azimutal grid connected to the RDF monitoring network developed by the Radio Emissions Project in collaboration with the Permanent Foundation G. Giuliani ONLUS and the University of Malaya. The image is divided into two parts: the upper part shows the world map of the RDF network developed by the authors; in the lower part is visible an enlargement of the epicentral area. The green marker represents the epicenter of M7.0 Russian earthquake which occurred on February 13, 2020 at 10:22:44 UTC. It is evident that, compared to the RDF monitoring network, the epicenter of the Russian earthquake is located between the yellow and green azimuths: this suggests that if pre-seismic electromagnetic emissions were generated through the direct piezoelectric effect in the focal zone of the Russian earthquake, these would appear on the RDF spectrograms as yellow-green spectrographic traces. Credits: Gabriele Cataldi, Daniele Cataldi, Giampaolo Gioacchino Giuliani, ZamriZainalAdibin, Radio Emissions Project.

Already from 23:00 UTC on 8 February 2020, at 07:30 UTC on 9 February 2020, a series of electromagnetic increases located at 0.001 Hz showed electromagnetic signals on the yellow/green azimuth (**Fig. 14**) from the first RDF station of Lariano (RM), Italy, about 9393km from the seismic epicenter. From the second RDF station of Lariano (RM), Italy, at 01:00 UTC on February 9, 2020 and at 06:50 UTC on February 10, 2020 other signals with the same azimuth were detected: these had a frequency between 0 and 4 Hz (**Fig. 15**).

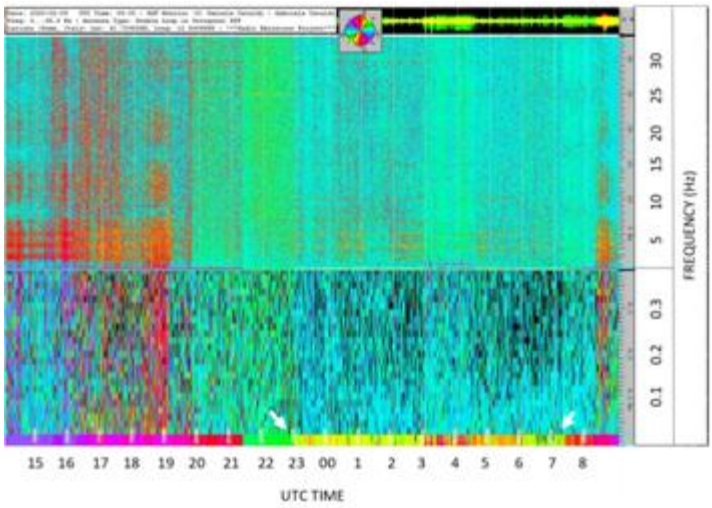

Fig. 14 – Spettrogramma dinamico realizzato dalla prima stazione RDF di Lariano (RM), Italy.

The dynamic spectrogram visible on the left was made by the first RDF monitoring station of Lariano (RM) between 8 and 9 February 2020. The white arrows indicate the spectrographic area where appeared the pre-seismic electromagnetic signals that have a compatible azimuth with the epicenter of M7.0 Russian earthquake. The UTC time relating to the recording of the spectrogram is shown on the X axis: this proceeds from right to left. The frequency of the monitored radio band is indicated on the Y axis: this is expressed in Hz. The spectrogram has been divided into two portions: the upper part highlights the ELF band; the lower part highlights the SELF band. Credits: Gabriele Cataldi, Daniele Cataldi, Radio Emissions Project.

Also from the second RDF station of Lariano (RM), Italy, at 03:40 UTC and at 04:40 UTC on 11 February 2020, a further electromagnetic peak was detected with the same azimuth (**Fig. 16**) and at a frequency between 0 and 4 Hz. From the spectral point of view, these radio emissions were found to be well detached from the natural electromagnetic background. Between 7 and 8 February 2020, the RDF monitoring station in Ripa Fagnano (AQ), Italy, detected other radio emissions (**Fig. 16-17**) with azimuth compatible with the epicenter of M7.0 Russian earthquake:

- an isolated electromagnetic peak around 13:00 UTC on 7 February 2020, having a frequency between 4 Hz and 11 Hz;
- a peak recorded between 01:00 UTC and 02:00 UTC on February 8, 2020, at a frequency between 0 and 6Hz;
- a large increase that began on February 8, 2020 at 03:00 UTC, at a frequency between 0 and 6 Hz.

On February 13, 2020, the same RDF station of Ripa-Fagnano (AQ), Italy, recorded intense emissions in the 0.1-12 Hz band, between 00:10 UTC and 07:50 UTC (**Fig. 17**). The signals lasted until the afternoon of

February 13, 2020, with a frequency between 0.2 Hz and 10 Hz (**Fig. 18**). The three RDF monitoring stations picked up a series of electromagnetic signals that had azimuth compatible with the geographical area in which the M7.0 Russian earthquake was subsequently recorded. In the preliminary phase of this result, the authors analyzed the azimuth data of the radio frequency monitored by the RDF monitoring network, verifying that the characteristics of the triangulation suggested that the seismic epicenter must have been far from the RDF stations: in fact, if the source of electromagnetic emission pre- seismic is located in the immediate vicinity of the RDF monitoring network, this will be correlated to a series of azimuth data that will result in several variables; conversely, a pre-seismic electromagnetic source located thousands of km from the RDF monitoring network will have less variable azimuth data between the RDF stations.

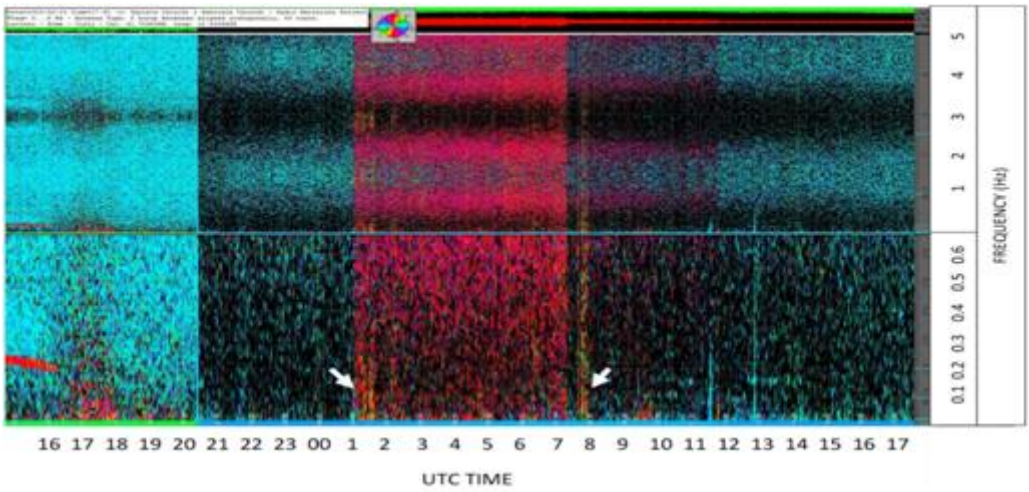

Fig. 15 – Dynamic spectrogram created by the second RDF station of Lariano (RM), Italy.

The dynamic spectrogram visible above was created by the first RDF monitoring station of Lariano on February 10, 2020. The white arrows indicate the spectrographic area where the pre-seismic electromagnetic signals appeared which have an azimuth compatible with the epicenter of M7.0 Russian earthquake. The UTC time relating to the recording of the spectrogram is shown on the X axis: this proceeds from right to left. The frequency of the monitored radio band is indicated on the Y axis: this is expressed in Hz. The spectrogram has been divided into two portions: the upper part highlights the ELF band; the lower part highlights the SELF band. Credits: Gabriele Cataldi, Daniele Cataldi, Radio Emissions Project.

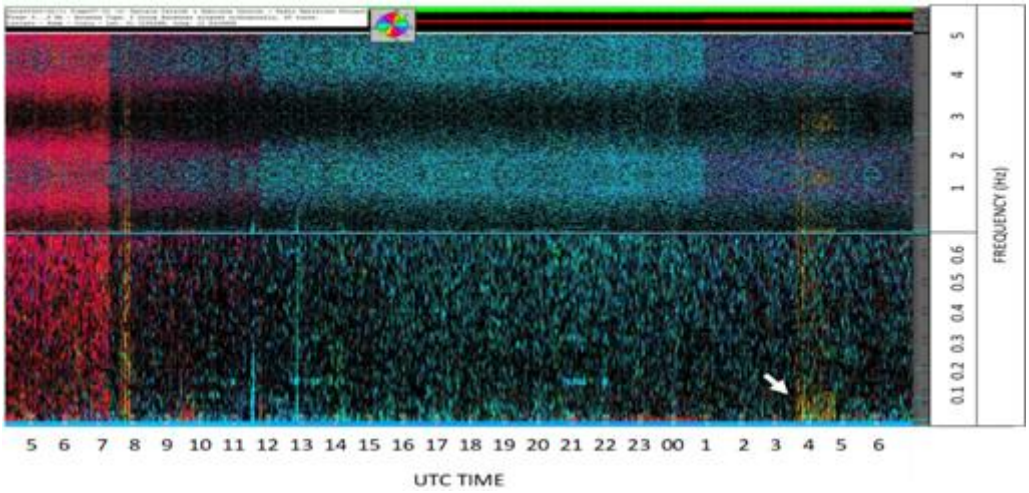

Fig. 16 – Dynamic spectrogram created by the second RDF station of Lariano (RM), Italy.

The dynamic spectrogram visible at the top was created by the first RDF monitoring station of Lariano (RM) on February 11, 2020. The white arrows indicate the spectrographic area where the pre-seismic electromagnetic signals appeared which have an azimuth compatible with the epicenter of M7.0 Russian earthquake. The UTC time relating to the recording of the spectrogram is shown on the X axis: this proceeds from right to left. The frequency of the monitored radio band is indicated on the Y axis: this is expressed in Hz. The spectrogram has been divided into two portions: the upper part highlights the ELF band; the lower part highlights the SELF band. Credits: Gabriele Cataldi, Daniele Cataldi, Radio Emissions Project.

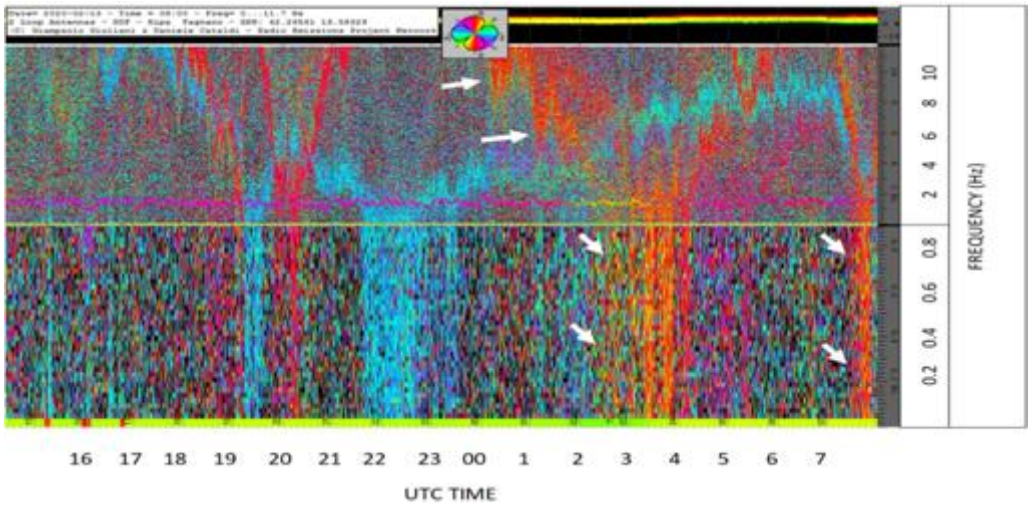

Fig. 17 – Dynamic spectrogram created by the RDF station of Ripa-Fagnano (AQ), Italy.

The dynamic spectrogram visible above was made by the RDF monitoring station of Ripa Fagnano (AQ) between 12 and 13 February 2020. The white arrows indicate the spectrographic area where the pre-seismic electromagnetic signals which have an azimuth compatible with the epicenter of M7.0 Russian earthquake. The UTC time relating to the recording of the spectrogram is shown on the X axis: this proceeds from right to left. The frequency of the monitored radio band is indicated on the Y axis: this is expressed in Hz. The spectrogram has been divided into two portions: the upper part highlights the ELF band; the lower part highlights the SELF band. Credits: Gabriele Cataldi, Daniele Cataldi, Radio Emissions Project.

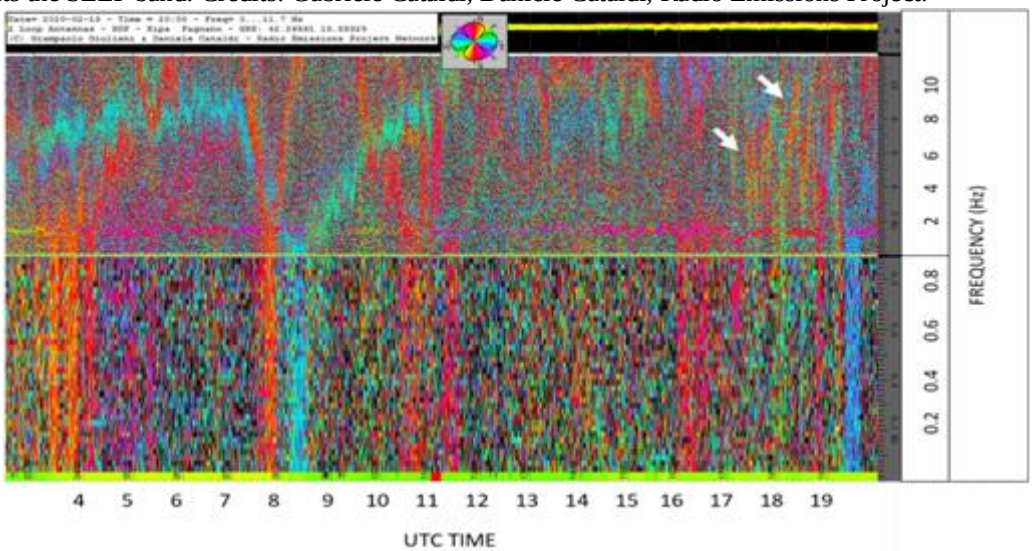

Fig. 18 – Dynamic spectrogram created by the RDF station of Ripa-Fagnano (AQ), Italy.

The dynamic spectrogram visible above was made by the RDF monitoring station of Ripa Fagnano (AQ) on February 13, 2020. The white arrows indicate the spectrographic area where the pre-seismic electromagnetic signals appeared which have an azimuth compatible with the epicenter of M7.0 Russian earthquake. The UTC time relating to the recording of the spectrogram is shown on the X axis: this proceeds from right to left. The frequency of the monitored radio band is indicated on the Y axis: this is expressed in Hz. The spectrogram has been divided into two portions: the upper part highlights the ELF band; the lower part highlights the SELF band. Credits: Gabriele Cataldi, Daniele Cataldi, Radio Emissions Project.

2.3 - Methods and data – M7.5 Russian earthquake

On 25 March 2020, at 02:49:25 UTC, an earthquake of magnitude Mw 7.5 was recorded at 221km SSE of Severo-Kuril'sk, Russia, with GPS (Global Positioning System) position: 48.964°N 157.696°E and at a depth of 57.8 km (**Fig. 19**).

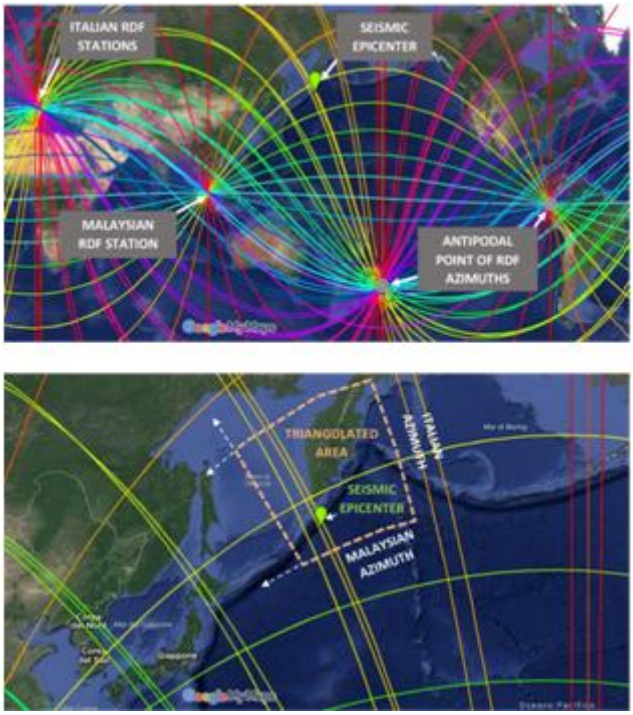

Fig. 19 – Analysis of the azimutal grid of the RDF monitoring network correlated to M7.5 Russian earthquake.

The image on the left shows the colorimetric map of the azimutal grid connected to the RDF monitoring network developed by the Radio Emissions Project in collaboration with the Permanent Foundation G. Giuliani ONLUS and the University of Malaya. The image is divided into two parts: the upper part shows the world map of the RDF network developed by the authors; in the lower part is visible an enlargement of the epicentral area. The green marker represents the epicenter of M7.5 Russian earthquake which occurred on March 25, 2020 at 02:49:25 UTC. It is evident that, compared to the RDF monitoring network, the epicenter of the Russian earthquake is located between the yellow and orange azimuths: this suggests that if pre-seismic electromagnetic emissions were generated through the direct piezoelectric effect in the focal zone of the Russian earthquake, these would appear on the RDF spectrograms as yellow-orange spectrographic traces. Credits: Gabriele Cataldi, Daniele Cataldi, Giampaolo Gioacchino Giuliani, ZamriZainalAdibin, Radio Emissions Project.

The M7.5 Russian earthquake was preceded by a series of electromagnetic emissions that were detected by the RDF monitoring network, allowing us to understand the azimuth of the seismic epicenter located thousands of kilometers away from the network itself. The first evidence of these pre-seismic electromagnetic emissions were recorded by the RDF station of Lariano (RM) (RDF Monitor 1) on March 22, 2020 between 03:00 UTC and 03:50 UTC, as shown in **Fig. 20**.

On the dynamic spectrogram, these radio signals are highlighted through a yellow azimuth, ie compatible with the epicentral area of the M7.5 earthquake (**Fig. 19**). In this case, the signals recorded had a frequency between 2.5 Hz and 7 Hz. Between 05:50 UTC and 07:40 UTC and again between 08:50 UTC and 11:00 UTC the same RDF survey station located in Lariano (RM), Italy, showed strong increases at a frequency of 0.001 Hz, right inside the geomagnetic band (as shown in **Fig. 20**) and on the same day (22 March 2020).

Other interesting registrations took place in the following days. Emissions on the same azimuth were always observed at a frequency of 0.001 Hz with the following times: 22:00 UTC and 23:50 on March 22, 2020; between 03:00 UTC and 05:00 UTC of 23 March 2020, with peaks distributed between 08:50 UTC and 16:10 UTC, at 17:00 UTC, between 18:00 UTC and 20:00 UTC, and again between 21:50 UTC and 22:30 UTC of the same day (as shown in **Fig. 20** and **Fig. 21**).

All these signals had an azimuth compatible with the seismic epicenter M7.5. Furthermore, the signals appeared again in the early hours of the following morning (March 24, 2020), around 07:30 UTC, and again between 09:30. UTC and 10:30 UTC, between 11:15 UTC and 13:30 UTC, a peak at 14:00 UTC and various

electromagnetic signals between 20:10 UTC and 21:30 UTC on March 24 2020 (as visible in **Fig. 22** and **Fig. 23**).

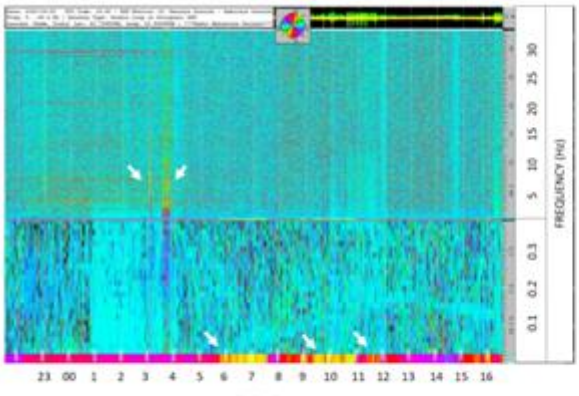

Fig. 20 – March 22, 2020

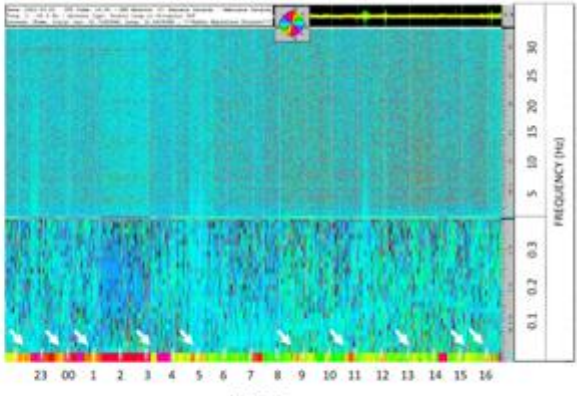

Fig. 21 – March 23, 2020

Fig. 20-21 – Dynamic spectrograms recorded by the RDF station of Lariano (RM), Italy - RDF Mnitor 1.

The spectrograms in the other show the sequence of the signals recorded in the electromagnetic spectrum monitored in the province of Rome, between 22 and 23 March 2020. The white arrows indicate the spectrographic area where appeared the pre-seismic electromagnetic signals that have a compatible azimuth with the epicenter of M7.5 Russian earthquake. The UTC time relating to the recording of the spectrogram is shown on the X axis: this proceeds from right to left. The frequency of the monitored radio band is indicated on the Y axis: this is expressed in Hz. The spectrogram has been divided into two portions: the upper part highlights the ELF band; the lower part highlights the SELF band. Credits: Gabriele Cataldi, Daniele Cataldi, Radio Emissions Project.

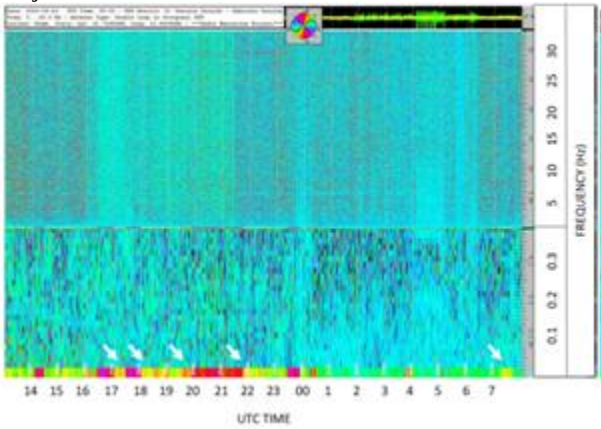

Fig. 22 – March 24, 2020

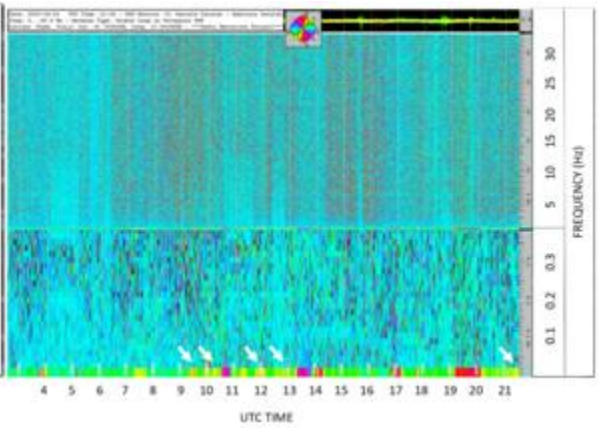

Fig. 23 – March 24, 2020

Fig. 22 -23 – Dynamic spectrograms recorded by the RDF station of Lariano (RM), Italy - RDF Mnitor 1.

The spectrograms above show the sequence of signals recorded in the electromagnetic spectrum monitored in the province of Rome, on 24 March 2020. The white arrows indicate the spectrographic area where appeared the pre-seismic electromagnetic signals that have a compatible azimuth with the epicenter of M7.5 Russian earthquake. The UTC time relating to the recording of the spectrogram is shown on the X axis: this proceeds from right to left. The frequency of the monitored radio band is indicated on the Y axis: this is expressed in Hz. The spectrogram has been divided into two portions: the upper part highlights the ELF band; the lower part highlights the SELF band. Credits: Gabriele Cataldi, Daniele Cataldi, Radio Emissions Project.

An isolated electromagnetic peak then appeared at the time of the earthquake (25 March 2020), maintaining the same epicentral azimuth, followed by a series of signals that showed variable azimuth for several hours (as shown in **Fig. 24**).

All these signals were recorded for several hours by the monitoring station located in the province of Rome, in Italy, but they were not the only phenomena of an electromagnetic nature to be observed before the M7.5 seismic event. Other equipment, in fact, always part of the RDF monitoring network developed by the Radio Emissions Project, showed electromagnetic increases correlated from the azimuthal point of view with the strong Russian seismic event.

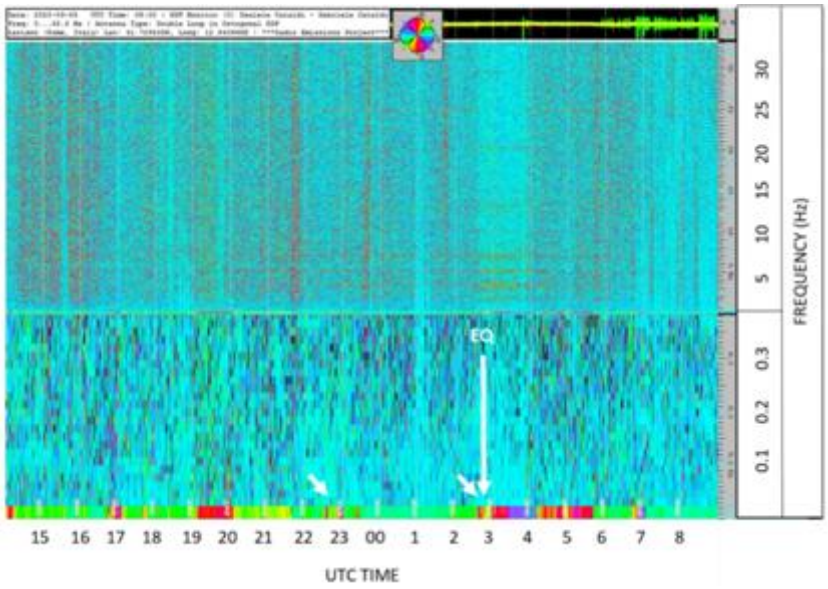

Fig. 24 – Dynamic spectrogram recorded by the RDF station of Lariano (RM), Italy - RDF Mnitor 1.

The spectrogram above shows the sequence of signals recorded in the electromagnetic spectrum monitored in the province of Rome, on 25 March 2020 close to the earthquake. The white arrows indicate the spectrographic area where appeared the pre-seismic electromagnetic signals that have a compatible azimuth with the epicenter of M7.5 Russian earthquake. The UTC time relating to the recording of the spectrogram is shown on the X axis: this proceeds from right to left. The frequency of the monitored radio band is indicated on the Y axis: this is expressed in Hz. The spectrogram has been divided into two portions: the upper part highlights the ELF band; the lower part highlights the SELF band. Credits: Gabriele Cataldi, Daniele Cataldi, Radio Emissions Project.

These signals appeared: between 18:00 UTC and 20:00 UTC on 24 March 2020, and shortly before the seismic shock: 02:10 UTC on 25 March 2020, remaining visible for a few hours even after the earthquake M7.5 (**Fig. 26**). The frequency of the electromagnetic signals recorded by the Ripa-Fagnano RDF station remained between 0.002 Hz and 11 Hz. The first radio signals were recorded at 18:30 UTC on 23 March 2020, followed by those that appeared between 23:00 UTC of 23 March 2020 and 08:00 UTC of 24 March 2020 (as shown in **Fig. 25**, **Fig. 26**). Other important signals were also recorded from the same station just before the earthquake as visible in the **Fig. 27**.

The importance of this recording was confirmed with other signals recorded by the other RDF monitoring stations, and not least the one located in Malaysia, managed by the University of Malaya (Kuala Lumpur). The signals were recorded starting from March 21, 2020, when they appeared at a frequency of 0.001 Hz, between the hours 17:50 UTC and the hours 00:00 UTC, also located on the same azimuth, that is the yellow/orange one (as visible in **Fig. 28**).

Through these signals, recorded by an RDF station located at a considerable distance from those in Italy, and precisely in the equatorial pacific area, it was possible to perform a precise triangulation of the radio signals between the following stations:

1. RDF Station of Lariano (RM), Italia.
2. RDF Station of Ripa-Fagnano (AQ), Italia.
3. RDF Station of Kuala Lumpur, Malesia.

The related data were able to identify a rectangular-shaped area of several thousand km^2, located N-E of Japan, right next to the future seismic epicenter (as visible in **Fig. 19**) on southern Pacific Russia.

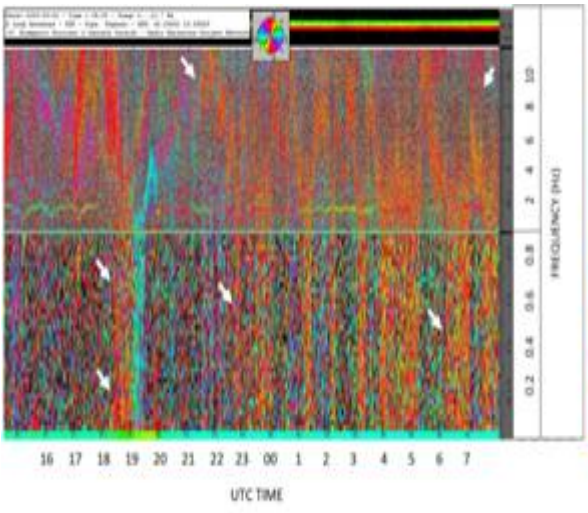

Fig. 25 – 23-24 Marzo 2020

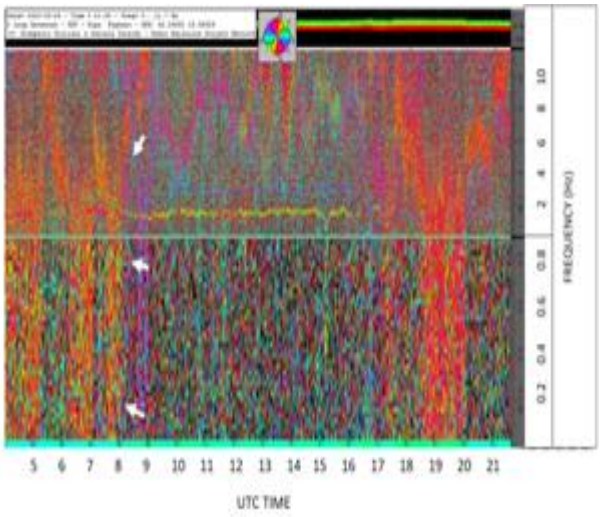

Fig. 26 – 24 Marzo 2020

Fig. 25-26 – Dynamic spectrograms recorded by the RDF station of Ripa-Fagnano (AQ), Italy.

The spectrograms above show the sequence of signals recorded in the electromagnetic spectrum monitored in the province of L'Aquila, between 23 and 24 March 2020 close to the earthquake. The white arrows indicate the spectrographic area where appeared the pre-seismic electromagnetic signals that have a compatible azimuth with the epicenter of M7.5 Russian earthquake. The UTC time relating to the recording of the spectrogram is shown on the X axis: this proceeds from right to left. The frequency of the monitored radio band is indicated on the Y axis: this is expressed in Hz. The spectrogram has been divided into two portions: the upper part highlights the ELF band; the lower part highlights the SELF band. Credits: Gabriele Cataldi, Daniele Cataldi, Radio Emissions Project.

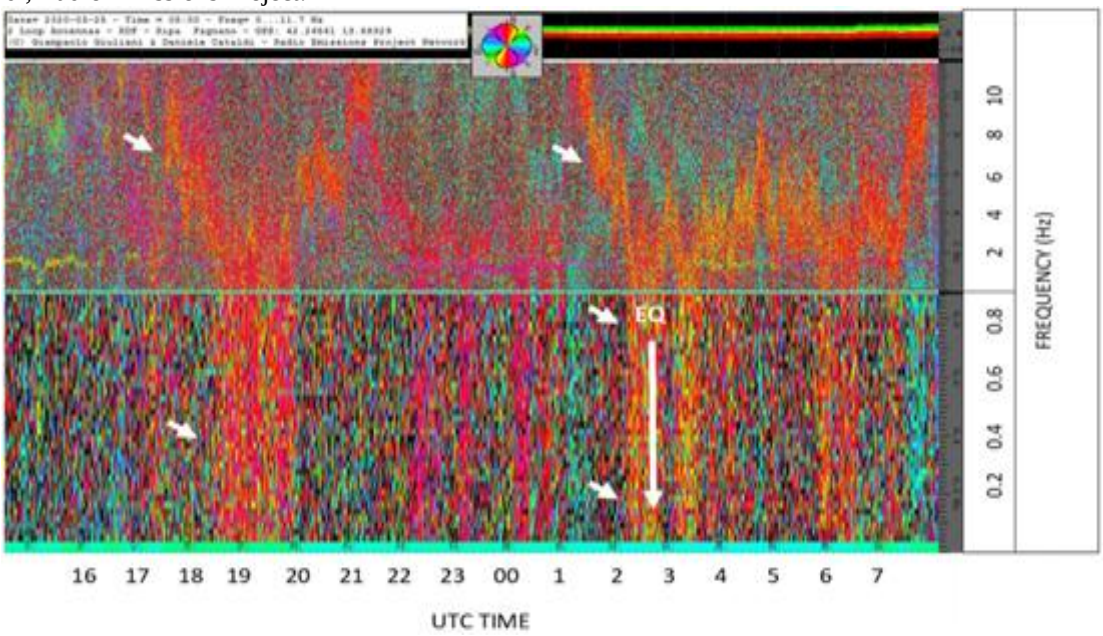

Fig. 27 – March 25, 2020

Fig. 27 – Dynamic spectrogram recorded by the RDF station of Ripa-Fagnano (AQ), Italy.

The spectrogram above shows the sequence of signals recorded in the electromagnetic spectrum monitored in the province of L'Aquila, on 25 March 2020 close to the earthquake. The white arrows indicate the spectrographic area where appeared the pre-seismic electromagnetic signals that have a compatible azimuth with the epicenter of M7.5 Russian earthquake. The UTC time relating to the recording of the spectrogram is shown on the X axis: this proceeds from right to left. The frequency of the monitored radio band is indicated on the Y axis: this is expressed in Hz. The spectrogram has been divided into two portions: the upper part highlights the ELF band; the lower part highlights the SELF band. Credits: Gabriele Cataldi, Daniele Cataldi, Radio Emissions Project.

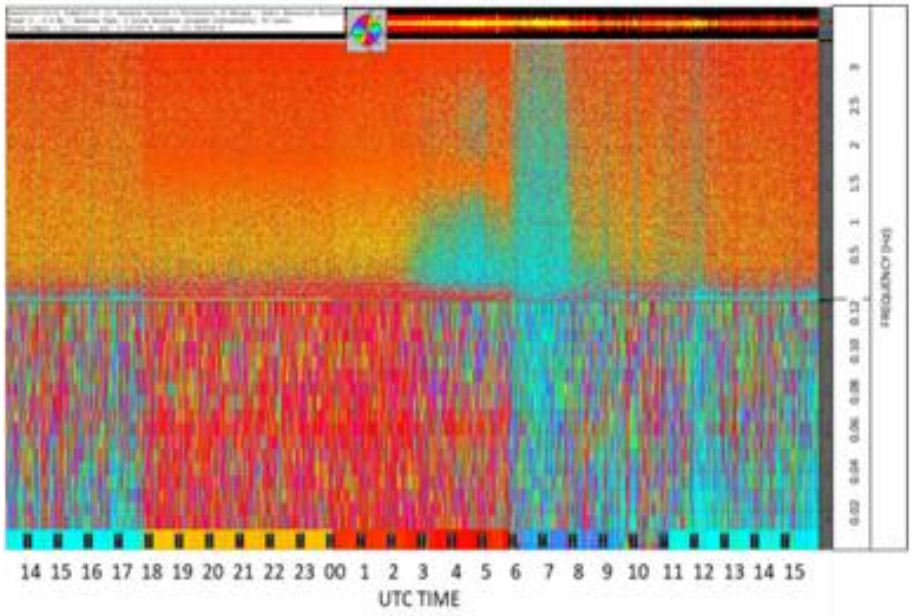

Fig. 28 – March 21, 2020

Fig. 28 – Dynamic spectrogram recorded by the RDF station of Kuala Lumpur, Malaysia.

The spectrogram shows the sequence of signals recorded in the electromagnetic spectrum monitored by the Malaysian station, on March 21, 2020 several days before the earthquake occurred. The orange signal, visible at the bottom of the spectrogram, indicates the pre-seismic electromagnetic signal that has azimuth compatible with the epicenter of M7.5 Russian earthquake. The UTC time relating to the recording of the spectrogram is shown on the X axis: this proceeds from right to left. The frequency of the monitored radio band is indicated on the Y axis: this is expressed in Hz. The spectrogram has been divided into two portions: the upper part highlights the ELF band; the lower part highlights the SELF band. Credits: Gabriele Cataldi, Daniele Cataldi, Radio Emissions Project.

Methods and data – M7.7 Jamaican earthquake data analysis

The analysis of the data from the set of dynamic spectrograms recorded by the RDF monitoring network developed by the Radio Emissions Project, highlights the behavior of pre-seismic radio anomalies of natural origin, having the azimuth of the seismic epicenter as a fundamental feature.

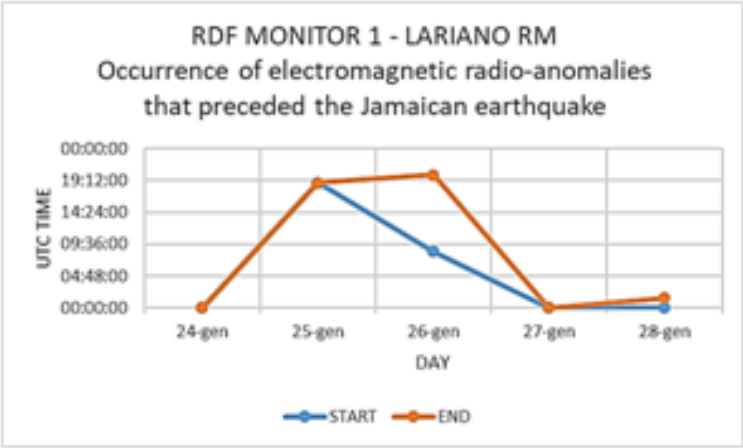

Fig. 29 – Occurrence of electromagnetic radio-anomalies that preceded the Jamaican earthquake – RDF monitor 1, Lariano (RM).

It highlights the appearance of radio anomalies, in relation to the time of appearance and the duration in days with respect to the seismic event that occurred on January 28, 2020. It is highlighted that in the vicinity of the seismic shock the time of appearance of the electromagnetic anomalies showed up during the night. Credits: Radio Emissions Project.

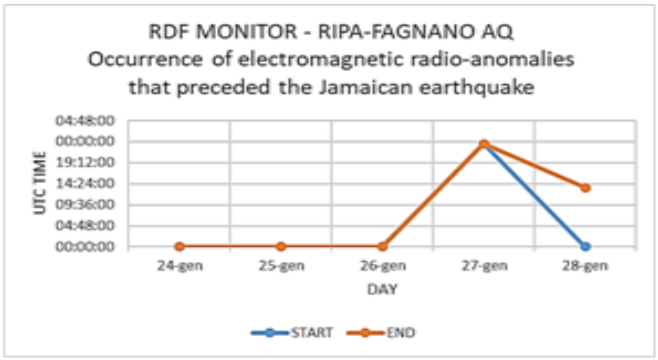

Fig. 30 – Occurrence of electromagnetic radio-anomalies that preceded the Jamaican earthquake – Ripa-Fagnano (AQ).

It highlights the time of appearance of the recorded radio anomalies, which, as can be seen, tend to appear in the evening before the seismic shock. The recording of the Ripa-Fagnano RDF station shows only an anomalous signal recorded during the day, on the day of the seismic shock, while the other radio anomalies always occurred during the night. Credits: Radio Emissions Project, Fondazione Permanente G. Giuliani.

Fig. 29 shows the appearance behavior of the radio anomalies recorded by the RDF monitoring station of Lariano (RM) (Monitor 1): the appearance of the pre-seismic radio anomalies occurred after a few days, while shortly before the seismic shock the appearance of the radio anomalies occurred during the night. In this context, even the RDF station of Ripa-Fagnano (AQ), almost always recorded anomalous electromagnetic signals at night before the seismic shock. Only one signal appears to have appeared during the day, as shown in **Fig. 30**.

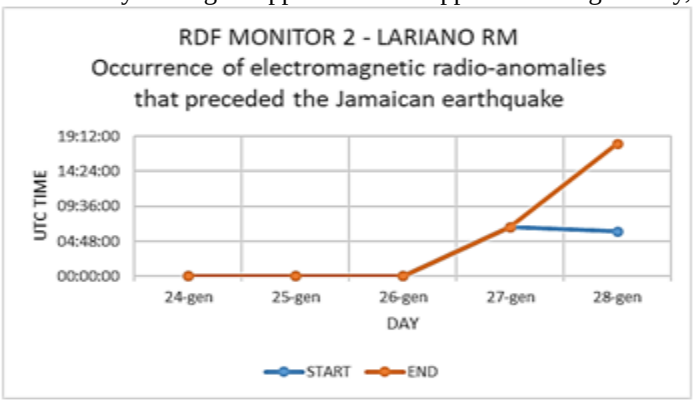

Fig. 31 – Occurrence of electromagnetic radio-anomalies that preceded the Jamaican earthquake – RDF monitor 2, Lariano (RM).

The graph above highlights the appearance of pre-seismic signals having azimuth compatible with that of the seismic epicenter. Also in this case the signals appeared mainly in the night/evening hours, and only a radio anomaly seems to appear during the day.. Credits: Radio Emissions Project.

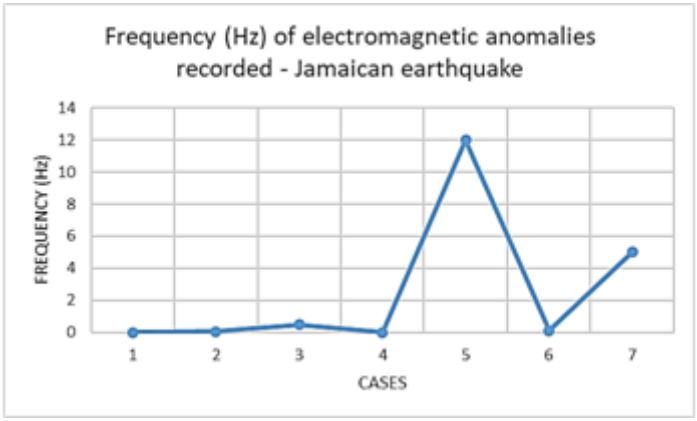

Fig. 32 – Graph of the variation of the frequency of natural radio electromagnetic signals recorded by the Italian RDF network.

It highlights how the majority of radio anomalies occur at a very low electromagnetic frequency. Credits: Radio Emissions Project.

As regards the M7.7 Jamaican earthquake, the pre-seismic radio anomalies correlated from the azimuth point of view to the epicentral geographic area seem to appear in the evening/night time, with only one exception recorded during the day (shortly before the alba), as seen in **Fig. 31**.

The analysis of the spectral fingerprints of the pre-seismic radio anomalies related to the Jamaican earthquake shows that the majority of these signals have a very low frequency (0.001 Hz - SELF band, >0-3 Hz or geomagnetic band); other pre-seismic radio anomalies have a higher frequency, albeit concentrated at a very low frequency, ie in the ELF band (3-30 Hz), as shown in **Fig. 32**. This type of radio emissions, thanks to their emission frequency (remarkably low), undergo a negligible level of attenuation as they pass through the propagation medium (earth's crust and atmosphere). Summing up:

- 71.4% of radio anomalies have an electromagnetic frequency close to 0.001 Hz;
- 28.6% of radio anomalies have an electromagnetic frequency between 7Hz and 12Hz.

The data extrapolated from the temporal context in which the radio anomalies appeared indicate that they appeared in the following way:

- 3 days before the earthquake.
- 2.41 days before the earthquake.
- 0.75 days before the earthquake.
- 1.16 days before the earthquake.
- 0.25 days before the earthquake.

From the date and times of appearance of each single electromagnetic emission it was possible to deduce how many days before these signals appeared before the Jamaican M7.7 seismic shock.

It follows that if we calculate the average of the 5 groups of radio anomalies that appeared on the dynamic spectrograms, we obtain an average of 1.5 days; average that corresponds to the time interval between the appearance of the pre-seismic radio anomalies and the seismic event related to them from the azimuthal point of view.

2.4 - Methods and data – M7.0Russian earthquake data analysis

As regards the analysis of the data relating to M7.0 Russian earthquake considered in this study (which took place on February 13, 2020), the monitoring data obtained by means of the RDF network developed and designed by the Radio Emissions Project, allowed to obtain very interesting.

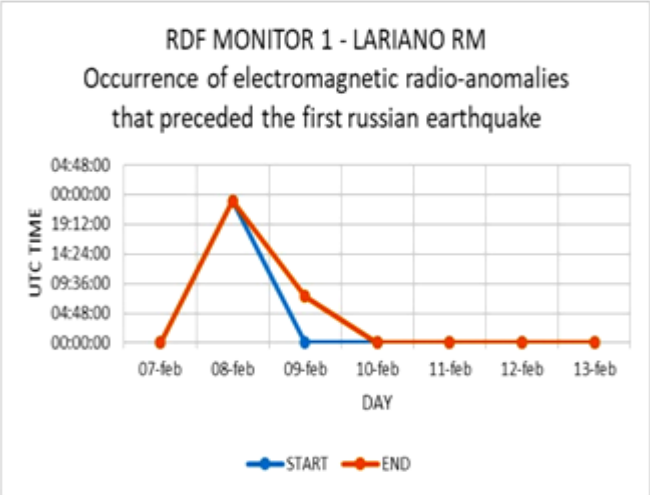

Fig. 33 – Occurrence of electromagnetic radio-anomalies that preceded the Russian earthquake – RDF monitor 1, Lariano (RM).

The graph above shows the time of appearance of the radio anomalies recorded before the earthquake occurrence. Credits: Radio Emissions Project.

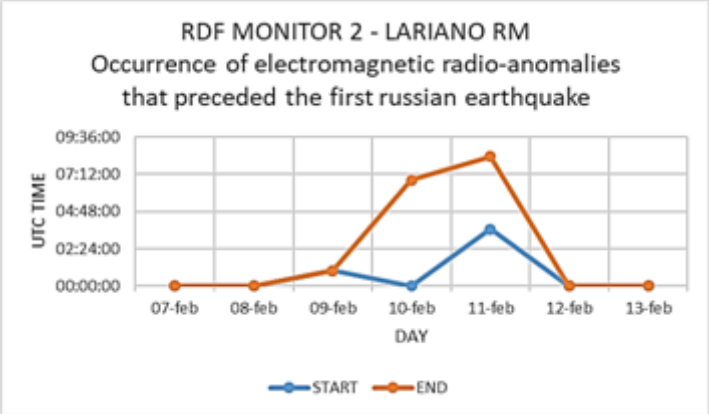

Fig. 34 – Occurrence of electromagnetic radio-anomalies that preceded the Russian earthquake – RDF monitor 2, Lariano (RM).

The graph above highlights the presence and appearance of radio anomalies before the seismic shock that occurred in Russia. The appearance of radio anomalies is observed in the evening or at night, and then reappears in the daytime, and reappears again at night, before the earthquake. Credits: Radio Emissions Project.

The evidence observed in **Fig. 33** provides interesting information to the researchers involved in the study: in this case the appearance of the pre-seismic radio anomalies recorded by means of the RDF monitoring station of Lariano (RM) occurred several days before the seismic shock , appearing in the evening hours and then reappearing and ending in the early hours of the next morning and again at night.
Also **Fig. 34** shows an identical trend of the phenomenon, even if it is a different RDF station. Also in this case, the pre-seismic radio anomalies recorded appear again a few days before the earthquake, in the evening/night time, reappearing in the daytime, until they reappear in the night hours just before the seismic shock. This indicates that it is a phenomenology of pre-seismic radio emissions that has characteristics that recur with a certain frequency before the seismic event related to them.

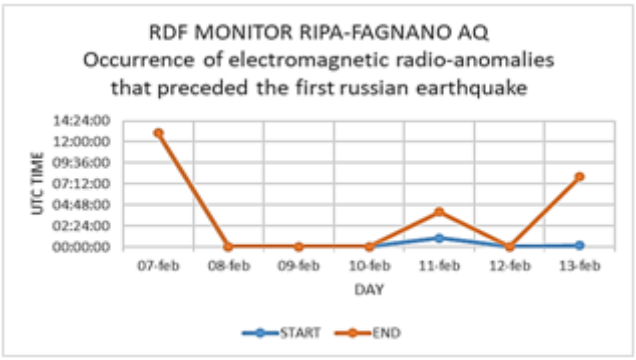

Fig. 35 – Occurrence of electromagnetic radio-anomalies that preceded the Russian earthquake – Ripa-Fagnano (AQ).

It indicates the evidence of electromagnetic increases several days before the seismic shock and at different times. Credits: Radio Emissions Project, Fondazione Permanente G. Giuliani.

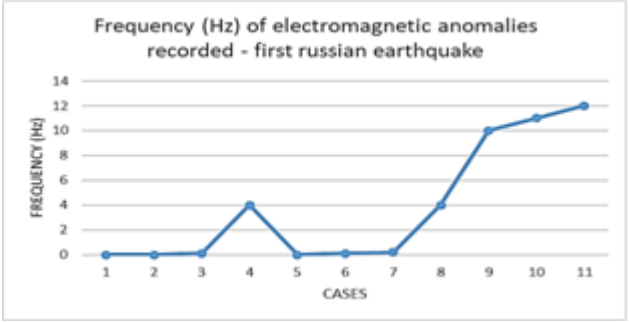

Fig. 36 – Graph of the variation of the frequency of natural radio electromagnetic signals, recorded by the Italian RDF network.

It highlights the trend of the appearance of electromagnetic signals with their relative frequency in Hz, before the occurrence of the Russian earthquake. Credits: Radio Emissions Project.

In the same period, another survey station highlighted pre-seismic electromagnetic signals having as their object the epicentral azimuth of the M7.0 earthquake that occurred in Russia. We are talking about the Ripa-Fagnano RDF station, located in Abruzzo (**Fig. 35**). **Fig. 36** highlights the frequency of the pre-seismic radio anomalies found before the M7.0 Russian earthquake by the Lariano (RM) RDF stations (RDF Monitor 1 and RDF Monitor 2) and by the RDF station of Ripa-Fagnano (AQ).

2.5 - Methods and data – M7.5 Russian earthquake data analysis

As for the analysis of the data obtained from the third case considered in this study, it refers to the second Russian earthquake of strong intensity, which occurred on March 25, 2020. This earthquake was also preceded by numerous pre-seismic electromagnetic increases but unlike of the other two cases already examined this earthquake recorded the appearance of a higher number of radio anomalies, as shown in **Fig. 37**.

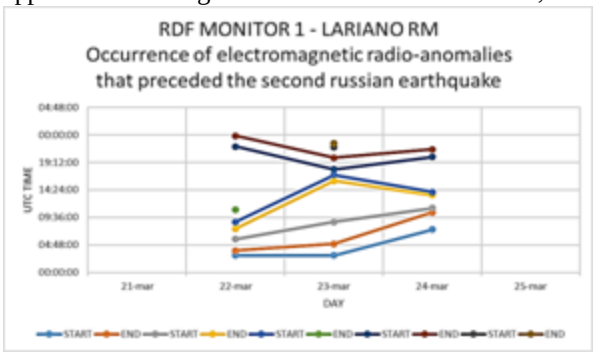

Fig. 37 – Occurrence of electromagnetic radio-anomalies that preceded the Russian earthquake – Lariano (RM).

It highlights the presence and appearance of numerous radio anomalies before the seismic shock that occurred in Russia. The appearance of radio anomalies is observed in the evening or night hours, but also vast electromagnetic increases appeared during the day. Credits: Radio Emissions Project.

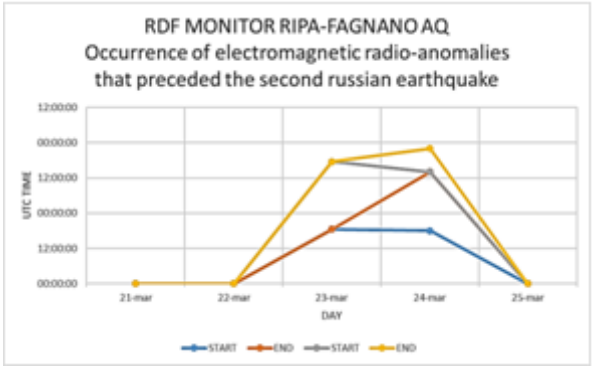

Fig. 38 – Graph of the data provided by the Ripa-Fagnano RDF monitoring station (AQ).

It highlights a large number of radio anomalies recorded between 3 and 1 days before the seismic shock. Credits: Radio Emissions Project, Fondazione Permanente G. Giuliani.

The analysis of the data relating to the monitoring of the Russian area highlighted, through **Fig. 37**, the appearance of numerous electromagnetic anomalies correlated from the azimuth point of view with the Russian M7.5 earthquake, which lasted several hours before the seismic shock. In this case, the appearance of the electromagnetic signals were concentrated in a particular time frame, i.e. between 4 and 3 days before the seismic shock:

- 8 radio-anomalies appeared on March 22, 2020.
- 9 radio-anomalies appeared on March 23, 2020.
- 7 radio-anomalies appeared on March 24, 2020.

A total of 24 radio anomalies

If we consider a total of three groups of electromagnetic emissions that appeared between 22 and 24 March 2020, they have distributed in the following percentage:

- 27,5 % on March 22, 2020.
- 33,3 % on March 23, 2020.
- 39,2 % on March 24, 2020.

The analysis of the recording of pre-seismic electromagnetic signals which took place in central Italy through the RDF station in Lariano (RM), highlighted that the majority of pre-seismic radio anomalies occurred on March 23, 2020, or the day before the seismic shock, as seen in **Fig. 37**.
According to what was recorded by the RDF station of Ripa-Fagnano (AQ), this earthquake was preceded by a large increase in radio anomalies as shown in **Fig. 38**; these emissions occurred between 3 and 1 days before the M7.5 seismic shock, almost all of which occurred in the evening/night hours. Out of 5 radio anomalies, 4 appeared at night and only one during the day:

- 80% of radio anomalies were recorded in the evening/night hours.
- 20% of radio anomalies were recorded in the time of maximum solar irradiation.

Once again, as observed in most cases, the radio anomalies then disappeared before the seismic shock (**Fig. 38**).
In this particular case of monitoring, a further and final reading of what happened before the seismic shock comes from the RDF monitoring station located in Malaysia, at the University of Malaya. In this case, the radio anomalies were observed on March 21, 2020, while the seismic shock occurred 4 days later, or March 25, 2020. The evidence of such data showed that very low frequency electromagnetic emissions only appeared in a restricted temporal context, namely March 21, 2020, as already mentioned and as visible in **Fig. 39**. In this particular case considered in the study, this last survey took place at a shorter distance than the other recordings as we are talking about an RDF station located in the peaceful area, or in the same area where the earthquake occurred.

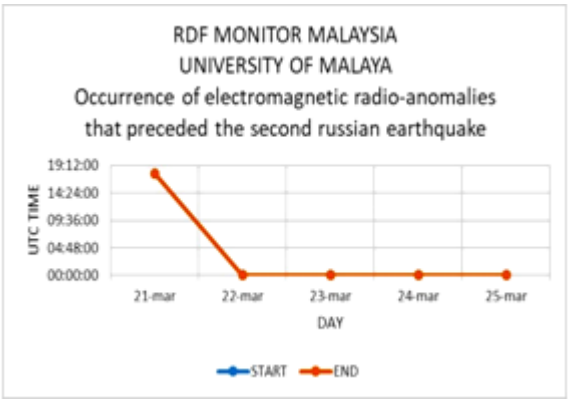

Fig. 39 – Graph made with data provided by the RDF monitoring station located in Kuala Lumpur, Malaysia, at the University of Malaya.

It highlights the presence of electromagnetic emissions having as their object the epicentral azimuth of the earthquake in Russia. Credits: Radio Emissions Project, Università di Malaya.

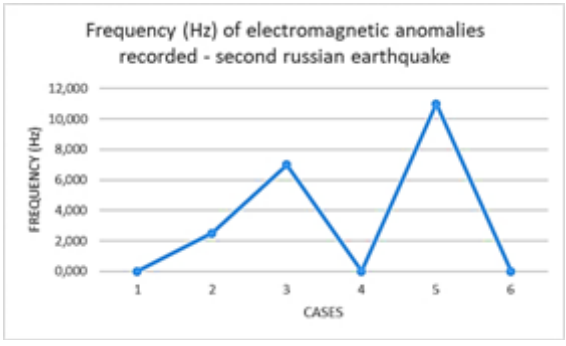

Fig. 40 – Graph of the frequency variation of natural radio electromagnetic signals, recorded by the world RDF network developed by the Radio Emissions Project.

It highlights the frequency of the recorded signals (in Hz). Once again a peak or increase in the electromagnetic frequency is visible before the seismic shock. Credits: Radio Emissions Project, Fondazione Permanente G. Giuliani, University of Malaya.

In this case the large difference in the number of data recorded by the Malaysian station, compared to the Italian stations, could depend on the shorter recording distance. Certainly, the characteristics of the Earth's crust in the focal area of the earthquake, the distance and characteristics of the ionosphere and solar activity can interfere with the propagation of electromagnetic signals.
Fig. 40 highlights the variation in frequency (Hz) of the recorded electromagnetic signals. It can be seen that before the seismic shock the electromagnetic frequency rises. Such emissions, therefore, always seem to increase in frequency before an earthquake occurs.

2.6 - Methods and data – Time of appearance of radio-anomalies

In this work it was found to be of fundamental importance to analyze the time of appearance of the radio anomalies related to the three M7+ seismic events considered to establish the time interval recorded between the appearance of the pre-seismic radio anomalies and the seismic event related to them.

❖ **M7.7 Jamaican Earthquake:**

The correlated time interval between the Jamaican earthquake and the RDF data provided by the Italian monitoring network reaches a maximum of 72 hours and a minimum of 7 hours (**Fig. 41**). If we analyze the total "average" distribution of the time intervals provided by each single RDF survey station located on the Italian territory, it is possible to obtain the average time intervals indicated in **Fig. 42**:

- 49.5 hours for the RDF Station located in Lariano (RM), Italy – (RDF Monitor 1).
- 25 hours for the RDF Station located in Ripa-Fagnano (AQ), Italy.
- 18.6 hours for the RDF Station located in Lariano (RM), Italy – (RDF Monitor 2).

Translated into hours (**Fig. 43**):

- 2.06 days for the RDF station of Lariano (RM), Italy (RDF Monitor 1).
- 1.04 days for the RDF station of Ripa-Fagnano (AQ), Italy.
- 0.75 days for the RDF station of Lariano (RM), Italy (RDF Monitor 2).

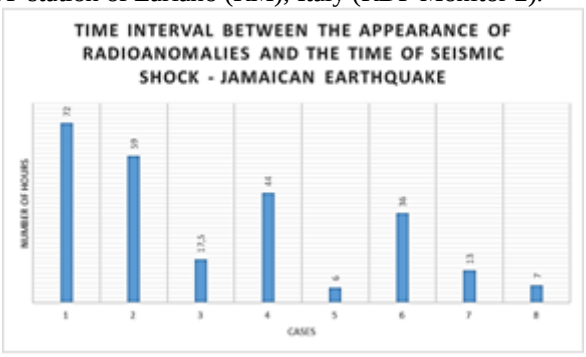

Fig. 41 – Hourly appearance of the radio anomalies recorded by the Italian RDF stations.

The graph above was created using the data provided by the RDF stations of Lariano (RM) and Ripa-Fagnano (AQ). Credits: Radio Emissions Project, Fondazione Permanente G. Giuliani.

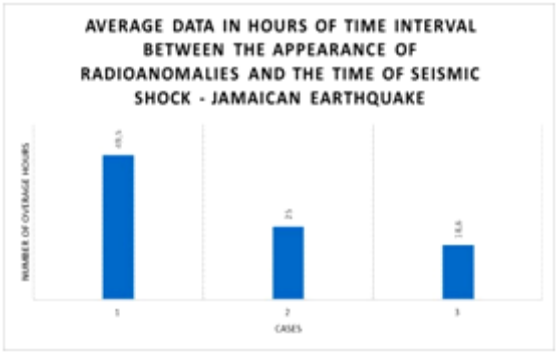

Fig. 42 – Average time intervals recorded by the Italian RDF network.

The graph above was created using the data provided by the RDF stations of Lariano (RM) and Ripa-Fagnano (AQ). Credits: Radio Emissions Project, Fondazione Permanente G. Giuliani.

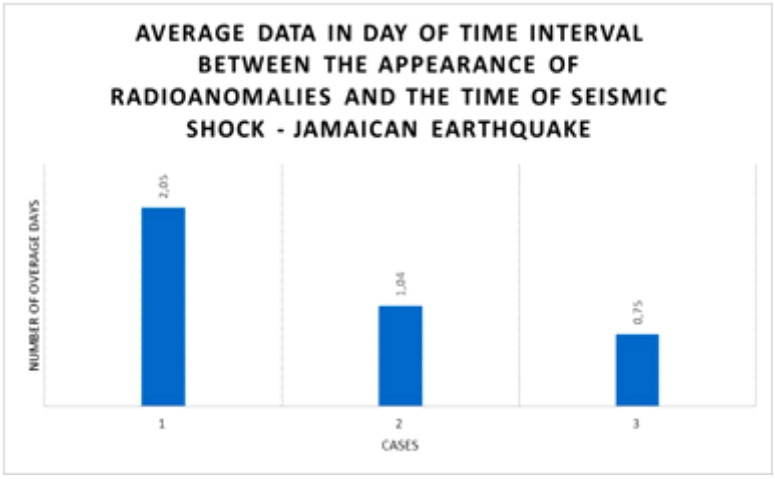

Fig. 43 – Average time intervals (in days) recorded by the Italian RDF network.

The graph above was created using the data provided by the RDF stations of Lariano (RM) and Ripa-Fagnano (AQ). Credits: Radio Emissions Project, Fondazione Permanente G. Giuliani.

The average time interval calculated using the data of all the Italian RDF stations is equal to 1.28 days.

❖ **M7.0 Russian earthquake:**

As for the M7.0 Russian earthquake recorded on 13 February 2020 at 10:22:44 UTC, the distribution of radio anomalies is of considerable interest. The total distribution in hours with respect to the time inteval between the time of appearance of the pre-seismic radio anomalies and the M7.0 Russian earthquake is visible in **Fig. 44**: the maximum time interval recorded is equal to 141 hours, while the minimum time interval recorded is 10 hours. As for the average in hours, of the time intervals recorded by the three RDF monitoring stations located on the Italian territory, the distribution is visible in **Fig. 45**:

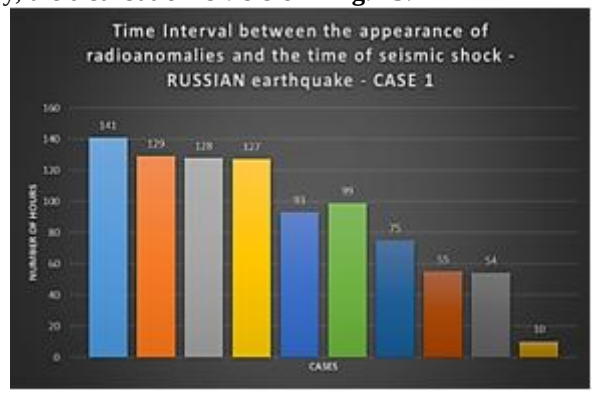

Fig. 44 – Hourly appearance of the radio anomalies recorded by the Italian RDF stations.

The graph above was created using the data provided by the RDF stations of Lariano (RM) and Ripa-Fagnano (AQ). Credits: Radio Emissions Project, Fondazione Permanente G. Giuliani.

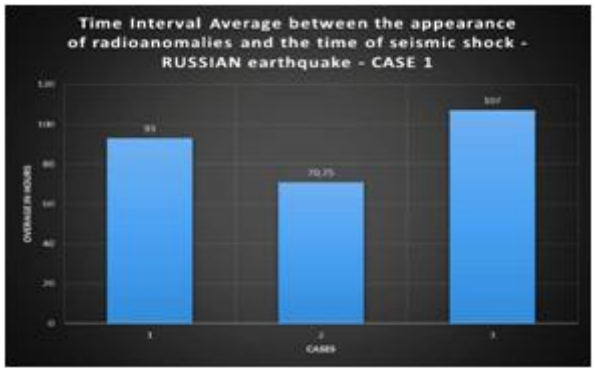

Fig. 45 – Average time intervals recorded by the Italian RDF network.

The graph above was created using the data provided by the RDF stations of Lariano (RM) and Ripa-Fagnano (AQ). Credits: Radio Emissions Project, Fondazione Permanente G. Giuliani.

In this case, the average time interval provided by the three RDF monitoring stations located on the Italian territory had a minimum duration of just under 3 days and a maximum of 4.45 days:

- 93 hours (3.87 days) before the seismic shock.
- 70.75 hours (2.94 days) before the seismic shock.
- 107 hours (4.45 days) before the seismic shock.

❖ **M7.5 Russian earthquake:**

As for the RDF related data at the M7.5 Russian earthquake recorded on March 25, 2020, at 02:49:25 UTC, the Italian monitoring stations recorded the first radio anomalies with azimuth compatible with the epicentral area well 72 hours before the M7.5 earthquake (**Fig. 46**).

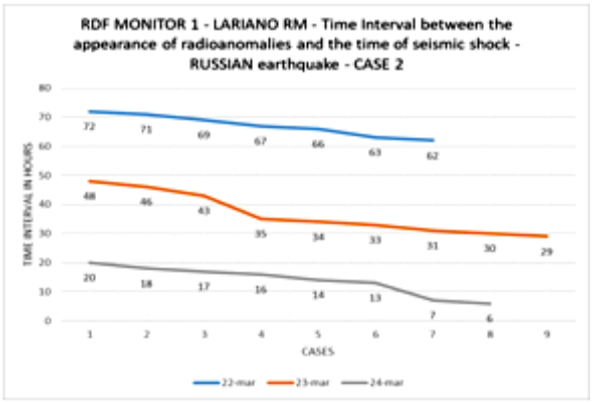

Fig. 46 –Hourly appearance of the radio anomalies recorded by the Italian RDF stations.

The graph above was created using the data provided by the RDF station located in Lariano (RM). Credits: Radio Emissions Project.

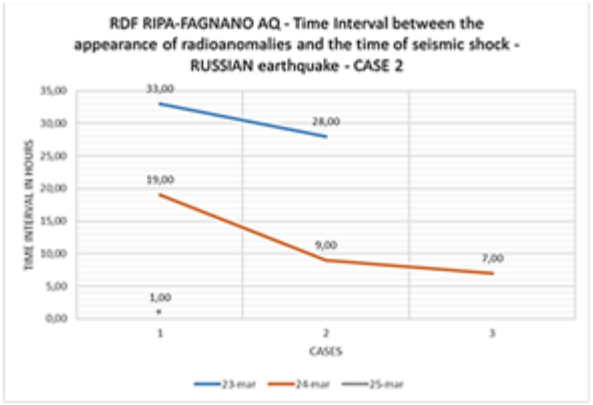

Fig. 47 –Average time intervals recorded by the Ripa-Fagnano (AQ) RDF station.

The graph above was created using the data provided by the RDF station located in Ripa-Fagnano (AQ). Credits: Radio Emissions Project, Fondazione Permanente G. Giuliani.

The RDF station of Lariano (RM) detected radiofrequency compatible with the epicentral area of the M7.5 earthquake with an advance ranging from 72 to 6 hours before the earthquake (**Fig. 46**). Other interesting data were provided by the RDF station of Ripa-Fagnano (AQ): this one detected radiofrequency compatible with the epicentral area of the M7.5 earthquake with an advance ranging from 33 to 1 hour before the earthquake (**Fig. 47**).

The last noteworthy recording comes from the RDF station located in the equatorial area, ie at the site of Kuala Lumpur, Malaysia (**Fig. 48**). In this case, the RDF station located on the Malaysian territory recorded radiofrequency compatible with the epicentral area of the M7.5 earthquake with an advance ranging from 82 to 75 hours before the seismic shock. The average time interval of the radio-anomalies was the following (**Fig. 49**):

- 37 hours – Lariano (RM) RDF Station – RDF Monitor 1.
- 16.16 hours – Ripa-Fagnano (AQ) RDF Station.
- 78.5 hours – Kuala Lumpur RDF Station, Malaya University, Malaysia.

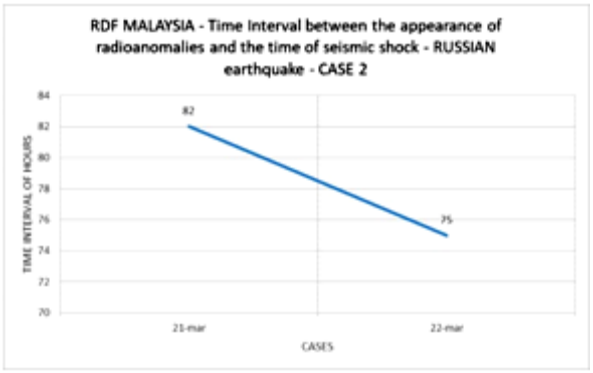

Fig. 48 – Hourly appearance of the radio anomalies recorded by the Kuala Lumpur RDF station, Malaya University, Malaysia.

The graph above was created using data provided by the RDF station located in Kuala Lumpur (Malaysia). Credits: Radio Emissions Project, University of Malaya.

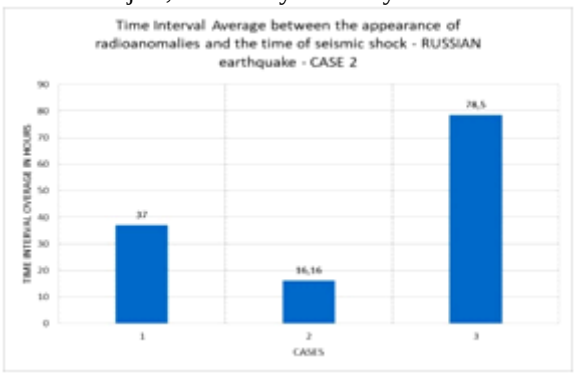

Fig. 49 – Average time intervals recorded by the RDF network.

The graph above was created using data provided by the Italian RDF stations and RDF station located in Kuala Lumpur (Malaysia). Credits: Radio Emissions Project, Fondazione Permanente G. Giuliani, University of Malaya.

This time interval is interesting, if converted into days:

- 1.54 days.
- 0.67 days.
- 3.27 days.

The average time interval calculated considering the data provided by all RDF stations located on a global scale is equivalent to:

- 1.82 days.

III. DISCUSSION

They can be detected in good time, of the electromagnetic emissions able to warn the occurrence of destructive earthquakes? In this context, the monitoring carried out by the researchers, by means of the RDF monitoring network, has enabled us to identify and follow the natural electromagnetic emissions and their trends over time, it has right now, suggested the occurrence of a strong earthquake.

As already explained during the discussion of these case studies, the appearance of the radio-anomalies is always associated with a limited temporal margin with respect to the appearance of strong destructive earthquakes; these signals are always signaled by the detection system, with the epicentral azimuth and this means that in these areas, before they are affected by a strong earthquake, are emitted electromagnetic signals of sufficient power to be detected on the entire globe.

Depending on the distance of detection, the type of weather cone and ionospheric characteristics, as well as the atmosphere itself, such signals have characteristics, but it is beyond all doubt, that these signals come from the areas within which a destructive quake presents.

The large amount of data, presented and treated extensively in previous chapters, it stresses that the RDF system allows to analyze these electromagnetic emissions, allowing, based on the morphology of these signals warn of the occurrence of a strong earthquake. This was seen clearly, for example, as regards the temporal scope of the appearances of these radio signals, also in relation to the variation of the electromagnetic frequency, but surely towards their direction of arrival (azimuth), with respect to the position of the future earthquake epicenter and the monitoring station that detected them.

There is no doubt that in such a monitoring context, the earthquakes are preceded by strong electromagnetic emissions, which is now possible to detect and monitor. With appropriate electronic and computerized system, these signals can be identified and it is possible to identify the geographical origin / crustal; will be used, however, other years, in order to define a safe and accurate monitoring system that may be able to indicate a precise area within which a strong intensity earthquake may occur, due to the amount of variables that still must be understood and that relate in generally the seismogenic on a global scale.

IV. CONCLUSIONS

The final figures, related to the study of the three destructive earthquakes considered in this study allow us to focus on the ability of the RDF monitoring network - Radio DirectionFinding, who was able to identify several days pre-seismic electromagnetic signals that occur before the earthquakes.
The three earthquakes considered are as follows:

- January 28, 2020, at 19:10:25 UTC - 7.7 MW located at 125 km NNW of Lucea, Jamaica, with GPS position (Global Positioning System): 19.440 ° N 78 755 ° W and at a depth of 10.0 km.
- February 13, 2020, at 10:22:44 UTC - 7.0 MW, located at 94 km ENE of Kuril'sk, Russia, with GPS position (Global Positioning System): 45 616 148 959 ° N ° E and 143.0 km.
- 25 March 2020 at 02:49:25 UTC - 7.5 MW, located 221 km SSE of Severo-Kurilsk, Russia, with GPS position (Global Positioning System): 48 964 157 696 ° N ° E and 57.8 km deep.

These earthquakes with a magnitude of minimum M7.0 and M7.7 maximum, then we speak of strong earthquakes, can produce widespread damage and many casualties. To mitigate the damage caused by the occurrence of these events is still a scientific challenge, but considering the electromagnetic type detections, acquired by means of the RDF monitoring network, developed by the Radio Emissions Project, it has been possible to ascertain, again, that before a strong earthquake, the earthquake epicenter and the lithosphere located in the immediate vicinity, emits radio frequency.
This radio is perceptible, trackable and measurable through the geomagnetic amplification system developed by the team of researchers. The analysis of these signals has always provided important information on the seismogenic in a global context since the first recordings obtained with such a monitoring network (March 2017).

The data tell us that on average, earthquakes have occurred several days after the onset of radio-abnormalities, specifically after:

- 1.5 days for the earthquake of January 28, 2020, Mw 7.7 located 125 km NNW of Lucea, Jamaica.
- 4.45 days for the earthquake of February 13, 2020, Mw 7.0, located 94 km ENE of Kuril'sk, Russia.
- 1.82 days for the earthquake of 25 March 2020, 7.5 w, located at 221 km SSE of Severo-Kurilsk, Russia.

This means that the Jamaican earthquake of January 28, 2020, could have been already identified 26 January 2020. That earthquake occurred in Kuril'sk, Russia February 13, 2020, could already be identified 9 February 2020, and that the quake of 25 March 2020, which occurred in Russia always Kuril'sk, it could already be expected on the evening of March 22, 2020.

From a forecasting perspective 1.5 days would be sufficient to alert a small geographical area, before a strong earthquake might strike. But the RDF network monitoring and forecasting technique developed by Radio Emissions Project, counts in this study is also a "time lag" of 4.45 days prior to a seismic shock. It is obvious that over four days notice might allow to secure a lot of people as well as to consider serious measures to maintain the technological facilities.

I therefore, data are very important, and indicate that the search must move forward, for the next few years, along this direction, in which the monitoring technique must be refined and improved.

The analysis of the data is evident, this indicates to us that the Precursors Seismic Electromagnetic SEPs, give the possibility to perform very precise forecast calculations (on a geographic surface), can be used to provide a seismic alert in the areas indicated by the monitoring system, which is able to identify the geographic area with a certain precision.

4.1 - Variability of the "Time Lag"

As regards the variation in hours of "time lag" in days, you are working to understand how there is never a high variable with certain earthquakes, compared to others. The answer may depend on the type of energy accumulation, the amount of electric charges involved on the fault plane, during the earthquake preparation, or the type of the same issue that can be isotropic or has a certain directivity (due to example the presence of water, obstacles, or even for the kind of rocks in which these charges are generated). Other variables can be derived definitely by the "fading" of the electromagnetic signal, especially over long distances, due to thunderstorms, ionospheric anomalies, defects in signal propagation, and anything else that may interfere with the propagation of radio signals.

Also on the front of the research, the study team has been working since 2017 to fully understand what kind of mechanism to determine this variability.

4.2 - Future development of the detection system

All researchers engaged in monitoring of natural geomagnetic bottom with this technological system, consider it important to develop in the coming years, a fully automated and computerized system based on RDF monitoring network, able to independently identify the possible Seismic Epicenter before it occurrence of a major earthquake. On this road, you're already working. Even the increase in the spread of a network of RDF detectors on a global scale, it can certainly mitigate any problems of detection of electromagnetic signals, being able to provide more data on which to work.

A greater number of data, provided by a more extended RDF monitoring network would provide more guidance on electromagnetic radio-triangulation of the recorded anomalies, increasing the accuracy of the detection system.

ACKNOWLEDGMENTS

A special thanks goes to those who have worked for the realization of such a detection system, not only in Italy, but also in Malaysia, for its continuous operation, among these:

- Angelo D'Errico - Foundation "G. Giuliani ONLUS ", L'Aquila, Italy - for his important contribution to the realization of the detection system in Italiy, Abruzzo.
- Shazwan Radzi - Radio Cosmology Research Lab, Department of Physics, University of Malaya - Kuala Lumpur, Malaysia - for its fundamental and irreplaceable aid in the management of the Malaysian RDF station.

REFERENCES

[1]. D. Cataldi, G. Cataldi and V. Straser. (2014). Variations of the Electromagnetic field that preceded the Peruvian M7.0 earthquake occurred on September 25, 2013. European Geosciences Union (EGU) General Assembly 2014, Geophysical Research Abstract, Vol. 16, Natural Hazard Section (NH4.3), Electro-magnetic phenomena and connections with seismo-tectonic activity, Vienna, Austria. Harvard-Smithsonian Center for Astrophysics, High Energy Astrophysics Division, SAO/NASA Astrophysics Data System.

[2]. D. Cataldi, G. Cataldi, V. Straser. (2017). SELF and VLF electromagnetic emissions that preceded the M6.2 Central Italy earthquake occurred on August 24, 2016. European Geosciences Union (EGU), General Assembly 2017. Seismology (SM1.2)/Natural Hazards (NH4.7)/Tectonics & Structural Geology (TS5.5) The 2016 Central Italy Seismic sequence: overview of data analyses and source models. Geophysical Research Abstracts Vol. 19, EGU2017-3675, 2017. Harvard-Smithsonian Center for Astrophysics, High Energy Astrophysics Division, SAO/NASA Astrophysics Data System.

[3]. D. Cataldi, G. Cataldi, V. Straser. (2019). Radio Direction Finding (RDF) - Pre-seismic signals recorded before the earthquake in central Italy on 1/1/2019 west of Collelongo (AQ). European

Geosciences Union (EGU) General Assembly 2019, Seismology (SM1.1) General Contributions on Earthquakes, Earth Structure, Seismology, Geophysical Research Abstract, Vol. 21, EGU2019-3124, 2019, Vienna, Austria. Harvard-Smithsonian Center for Astrophysics, High Energy Astrophysics Division, SAO/NASA Astrophysics Data System.

[4]. D. Cataldi, G. G. Giuliani, V. Straser, G. Cataldi. (2020). Radio signals and changes of flow of Radon gas (Rn222) which led the seismic sequence and the earthquake of magnitude Mw 4.4 that has been recorded in central Italy (Balsorano, L'Aquila) on November 7, 2019. An international journal for New Concepts in Geoplasma Tectonics, Volume 8, Number 1, May 2020, pp. 32-42.

[5]. D. Finkelstein, U. S. Hill, J. R. Powell. (1973). The piezoelectric theory of earthquake lightning. J. Geophys. Res., 78, 992-993.

[6]. D. V. Reames, Astrophysical J. 571, L63 (2002).

[7]. F. Di Stefano, G. Giuliani, D. Ouzounov, D. Cataldi, C. Fidani, A. D'Errico, G. Fioravanti. (2020). Support for preventions and preparedness of the strait of Messina.Reggio Calabria – An earthquake forecasting project. Atti della Accademia Peloritana dei Pericolanti Classe di Scienze Fisiche, Matematiche e Naturali. May 4, 2020.

[8]. F. Freund. (2002). Charge generation and propagation in igneous rocks. Special Issue of the Fournal of Geodynamics. NASA Ames Research Center; Moffett Field, CA United States.

[9]. G. Cataldi, D. Cataldi, V. Straser. (2013). Variations Of Terrestrial Geomagnetic Activity Correlated To M6+ Global Seismic Activity. EGU (European Geosciences Union) 2013, General Assembly, Seismology Section (SM3.1), Earthquake precursors, bio-anomalies prior to earthquakes and prediction, Geophysical Research Abstracts, Vol. 15. Vienna, Austria. Harvard-Smithsonian Center for Astrophysics, High Energy Astrophysics Division, SAO/NASA Astrophysics Data System.

[10]. G. Cataldi, D. Cataldi and V. Straser. (2014). Earth's magnetic field anomalies that precede the M6+ global seismic activity. European Geosciences Union (EGU) General Assembly 2014, Geophysical Research Abstract, Vol. 16, Vienna, Austria. Natural Hazard Section (NH4.3), Electro-magnetic phenomena and connections with seismo-tectonic activity, Harvard-Smithsonian Center for Astrophysics, High Energy Astrophysics Division, SAO/NASA Astrophysics Data System.

[11]. G. Cataldi, D. Cataldi, V. Straser. (2015). Solar wind proton density variations that preceded the M6+ earthquakes occurring on a global scale between 17 and 20 April 2014. European Geosciences Union (EGU) General Assembly 2015, Vienna, Austria. Natural Hazard Section (NH5.1), Sea & Ocean Hazard - Tsunami, Geophysical Research Abstract, Vol. 17, Harvard-Smithsonian Center for Astrophysics, High Energy Astrophysics Division, SAO/NASA Astrophysics Data System.

[12]. G. Cataldi, D. Cataldi, V. Straser. (2015). Solar wind ion density variations that preceded the M6+ earthquakes occurring on a global scale between 3 and 15 September 2013. European Geosciences Union (EGU) General Assembly 2015, Geophysical Research Abstract, Vol. 17, Vienna, Austria. Natural Hazard Section (NH5.1), Sea & Ocean Hazard - Tsunami, Harvard-Smithsonian Center for Astrophysics, High Energy Astrophysics Division, SAO/NASA Astrophysics Data System.

[13]. G. Cataldi, D. Cataldi, V. Straser. (2015). Solar wind proton density variations that preceded the M6,1 earthquake occurred in New Caledonia on November 10, 2014. European Geosciences Union (EGU) General Assembly 2015, Geophysical Research Abstract, Vol. 17, Vienna, Austria. Natural Hazard Section (NH5.1), Sea & Ocean Hazard - Tsunami, Harvard-Smithsonian Center for Astrophysics, High Energy Astrophysics Division, SAO/NASA Astrophysics Data System.

[14]. G. Cataldi, D. Cataldi, V. Straser. (2016). Solar activity correlated to the M7.0 Japan earthquake occurred on April 15, 2016. New Concepts in Global Tectonics Journal, V. 4, No. 2, June 2016.

[15]. G. Cataldi, D. Cataldi, V. Straser. (2016). Tsunami related to solar and geomagnetic activity. European Geosciences Union (EGU) General Assembly 2016, Natural Hazard Section (NH5.6), Complex modeling of earthquake, landslide, and volcano tsunami sources. Geophysical Research Abstract, Vol. 18, Vienna, Austria. Harvard-Smithsonian Center for Astrophysics, High Energy Astrophysics Division, SAO/NASA Astrophysics Data System.

[16]. G. Cataldi, D. Cataldi, V. Straser. (2017). SELF-VLF electromagnetic signals and solar wind proton density variations that preceded the M6.2 Central Italy earthquake on August 24, 2016. International Journal of Modern Research in Electrical and Electronic Engineering, Vol. 1, No. 1, 1-15, 2017. DOI: 10.20448/journal.526/2017.1.1/526.1.1.15.Harvard-Smithsonian Center for Astrophysics, High Energy Astrophysics Division, SAO/NASA Astrophysics Data System.

[17]. G. Cataldi, D. Cataldi, V. Straser. (2017). Solar and Geomagnetic Activity Variations Correlated to Italian M6+ Earthquakes Occurred in 2016. European Geosciences Union (EGU), General Assembly 2017. Geophysical Research Abstracts Vol. 19, EGU2017-3681, 2017. Seismology (SM1.2)/Natural Hazards (NH4.7)/Tectonics & Structural Geology (TS5.5) The 2016 Central Italy Seismic sequence:

overview of data analyses and source models.Harvard-Smithsonian Center for Astrophysics, High Energy Astrophysics Division, SAO/NASA Astrophysics Data System.

[18]. G. Cataldi, D. Cataldi, V. Straser. (2017). Solar wind proton density increase that preceded Central Italy earthquakes occurred between 26 and 30 October 2016. European Geosciences Union (EGU), General Assembly 2017. Geophysical Research Abstracts Vol. 19, EGU2017-3774, 2017. Seismology (SM1.2)/Natural Hazards (NH4.7)/Tectonics & Structural Geology (TS5.5) The 2016 Central Italy Seismic sequence: overview of data analyses and source models. Harvard-Smithsonian Center for Astrophysics, High Energy Astrophysics Division, SAO/NASA Astrophysics Data System.

[19]. G. Cataldi, D. Cataldi, V. Straser. (2019). Solar wind ionic density variations related to M6+ global seismic activity between 2012 and 2018. European Geosciences Union (EGU) General Assembly 2019, Short-term Earthquake Forecast (StEF) and multy-parametric time-Dependent Assessment of Seismic Hazard (t-DASH) (NH4.3/AS4.62/EMRP2.40/ESSI1.7/Gi2.13/SM3.9), General Contribution on Earthquakes, Earth Structure, Seismology (SM1.1), Geophysical Research Abstract, Vol. 21, EGU2019-3067, 2019, Vienna, Austria. Harvard-Smithsonian Center for Astrophysics, High Energy Astrophysics Division, SAO/NASA Astrophysics Data System.

[20]. G. Cataldi, D. Cataldi, V. Straser. (2019). Wolf Number Related To M6+ Global Seismic Activity. New Concepts in Global Tectonics Journal, Volume 7, Number 3, December 2019, pp. 179-186.

[21]. G. Cataldi. (2020). Precursori Sismici – Monitoraggio Elettromagnetico. Kindle-Amazon, ISNB: 9798664537970. ASIN Code: B08CPDBGX9.

[22]. J. A. Broun. (1861). On the horizontal force of the Earth's magnetism, Proc. Roy. Soc. Edinburgh, 22, 511.

[23]. K. Ohta, J. Izutsu, A. Schekotov, and M. Hayakawa (2013), The ULF/ELF electromagnetic radiation before the 11 March 2011 Japanese earthquake, Radio Sci., 48, 589–596, doi:10.1002/rds.20064.

[24]. N. A. F. Moos. (1910). Magnetic observations made at the government observatory, Bombay, for the period 1846 to 1905, and their discussion, Part II: the phenomenon and its discussion, Bombay.

[25]. T. Rabeh, G. Cataldi, V. Straser. (2014). Possibility of coupling the magnetosphere–ionosphere during the time of earthquakes. European Geosciences Union (EGU) General Assembly 2014, Geophysical Research Abstract, Vol. 16, Vienna, Austria. Natural Hazard Section (NH4.3), Electro-magnetic phenomena and connections with seismo-tectonic activity. Harvard-Smithsonian Center for Astrophysics, High Energy Astrophysics Division, SAO/NASA Astrophysics Data System.

[26]. V. Straser. (2011). Radio Wave Anomalies, Ulf Geomagnetic Changes And Variations In The Interplanetary Magnetic Field Preceding The Japanese M9.0 Earthquake. New Concepts in Global Tectonics Newsletter, no. 59, June, 2011. Terenzo PR, Italy.

[27]. V. Straser. (2011). Radio Anomalies And Variations In The Interplanetary Magnetic Field Used As Seismic Precursor On A Global Scale, New Concepts in Global Tectonics Newsletter, no. 61, December, 2011. Terenzo PR, Italy.

[28]. V. Straser. (2012). Can IMF And The Electromagnetic Coupling Between The Sun And The Earth Cause Potentially Destructive Earthquakes? New Concepts in Global Tectonics Newsletter, no. 65, December, 2012. Terenzo PR, Italy. Society for Interdisciplinary Studies (SIS).

[29]. V. Straser. (2012). Intervals Of Pulsation Of Diminishing Periods And Radio Anomalies Found Before The Occurrence of M6+ Earthquakes. New Concept in Global Tectonics Newsletter, no. 65, December, 2012. Terenzo PR, Italy.

[30]. V. Straser, G. Cataldi. (2014). Solar wind proton density increase and geomagnetic background anomalies before strong M6+ earthquakes. Space Research Institute of Moscow, Russian Academy of Sciences, MSS-14. 2014. Moscow, Russia.

[31]. V. Straser, G. Cataldi. (2015). Solar wind ionic variation associated with earthquakes greater than magnitude M6.0. New Concepts in Global Tectonics Journal, V. 3, No. 2, June 2015, Australia. P.140-154.

[32]. V. Straser, G. Cataldi, D. Cataldi. (2015). Solar wind ionic and geomagnetic variations preceding the Md8.3 Chile Earthquake. New Concepts in Global Tectonics Journal, V. 3, No. 3, September 2015, Australia. P.394-399.

[33]. V. Straser, G. Cataldi, D. Cataldi. (2016). SELF and VLF electromagnetic signal variations that preceded the Central Italy earthquake on August 24, 2016. New Concepts in Global Tectonics Journal, V. 4, No. 3, September 2016. P.473-477. Harvard-Smithsonian Center for Astrophysics, High Energy Astrophysics Division, SAO/NASA Astrophysics Data System.

[34]. V. Straser, G. Cataldi, D. Cataldi. (2017). Solar and electromagnetic signal before Mexican Earthquake M8.1, September 2017. New Concepts in Global Tectonics Journal, V. 5, No. 4, December 2017.

[35]. V. Straser. (2017). Plasmas in the atmosphere, tectonics and earthquake: a possible link for the crustal diagnosis? American Geophysical Union, Fall Meeting 2017, abstract #NH21C-0178.

[36]. V. Straser, D. Cataldi, G. Cataldi. (2018). Radio Direction Finding System, a new perspective for global crust diagnosis. New Concepts in Global Tectonics Journal, V. 6, No. 2, June 2018.

[37]. V. Straser, H. Wu, A. Bapat, N. Venkatanathan, Z. Shou, G. Gregori, B. Leybourne, L. Hissink. (2019) Multi-parametric Earthquake Forecasting From Electromagnetic Coupling between Solar Corona and Earth System Precursors. 21st EGU General Assembly, EGU2019, Proceedings from the conference held 7-12 April, 2019 in Vienna, Austria, id.5976. Harvard-Smithsonian Center for Astrophysics, High Energy Astrophysics Division, SAO/NASA Astrophysics Data System.

[38]. V. Straser, D. Cataldi, G. Cataldi. (2019). Registration of Pre-Seismic Signals Related to the Mediterranean Area with the Rdf System Developed by the Radio Emissions Project. International Journal of Engineering Science Invention (IJESI), www.ijesi.org. Volume 8 Issue 03 Series. March 2019. PP 26-35. ISSN (Online): 2319 – 6734, ISSN (Print): 2319 – 6726. 2019.

[39]. V. Straser, D. Cataldi, G. Cataldi. (2019). Radio Direction Finding (RDF) - Geomagnetic Monitoring Study of the Himalaya Area in Search of Pre-Seismic Electromagnetic Signals. Asian Review of Environmental and Earth Sciences, v. 6, n. 1, p. 16-27, 14 jun. 2019

[40]. V. Straser, D. Cataldi, G. Cataldi. (2019). Electromagnetic monitoring of the New Madrid fault us area with the RDF system - Radio Direction Finding of the radio emissions project. New Concepts in Global Tectonics Journal, V7 N1, March 2019.

[41]. V. Straser, G. Cataldi, D. Cataldi. (2019). Namazu's Tail – RDF: a new perspective for the study of seismic precursors of Japan. Lulu Editore, 2019.

[42]. V. Straser, G. G. Giuliani, D. Cataldi, G. Cataldi. (2020). Multi-parametric investigation of pre-seismic origin phenomena through the use of RDF technology (Radio Direction Finding) and the monitoring of Radon gas stream (RN222). An international journal for New Concepts in Geoplasma Tectonics, Volume 8, Number 1, May 2020, pp. 11-27.

[43]. W. G. Adams. (1982). Comparison of simultaneous magnetic disturbance at several observatories, Phil. Trans. London (A), 183, 131.